WHC-EP--0065

DE89 000691

Electrochemical Corrosion-Scoping Experiments-- An Evaluation of the Results

H. D. Smith

Date Published
September 1988

Prepared for the U.S. Department of Energy
Office of Civilian Radioactive Waste Management

Westinghouse Hanford Company
P.O. Box 1970
Richland, Washington 99352

Hanford Operations and Engineering Contractor for the
U.S. Department of Energy under Contract DE-AC06-87RL10930

Nevada Nuclear Waste Storage Investigations Prepared by NNWSI Project participants as part of the Civilian Radioactive Waste Management Program (CRWM). The NNWSI Project is managed by the Waste Management Project Office (WMPO) of the USDOE, Nevada Operations Office (DOE/NV). NNWSI Project work is sponsored by the Office of Geologic Repositories (OGR) of the USDOE, Office of Civilian Radioactive Waste Management (OCRWM).

ACKNOWLEDGMENTS

The author wishes to acknowledge Dale Archer of Analytical Chemistry for running the experiments. Jack McCarthy of Physical Metallurgy performed the transmission electron microscopy and electron diffraction work on the archive specimen and the 12-month experiment specimen.

CONTENTS

FIGURES

FIGURES (Cont'd)

TABLES

ELECTROCHEMICAL CORROSION SCOPING EXPERIMENTS-- AN EVALUATION OF THE RESULTS

I. SUMMARY

Prior to emplacement in a nuclear waste repository, each waste form must be well characterized with respect to its behavior in the environments expected to develop in the repository. This scoping study was designed to obtain a qualitative idea of how spent fuel cladding would respond to a hot water environment that could develop in a tuff repository at a time when temperatures have cooled to ~95 °C and hot liquid water has infiltrated the repository horizon. That information would then be used to establish more definitive tests on cladding behavior in a tuff repository.

For this study bundles of spent fuel cladding held together with a 304 stainless steel (SS) wrap were constructed which simulate the geometries and materials associations in a breached 304L SS container. They were exposed to 90 °C tuff-equilibrated Well J-13 water for periods of 2, 6, and 12 mo.

During the experiments, the water level, temperature, conductivity, and pH were monitored on a regular basis. The water was also checked periodically for carbon (organic, inorganic, and later in the experiment Carbon-14) and zirconium. More extensive water analyses were carried out at the midpoint and completion of the experiments.

Several lines of specimen evaluation indicated no detectable or very limited corrosion had occurred in any of the rod sections. Patterns created by black (pretransition) and gray (posttransition) oxide films in transition areas showed no change as a result of the 6-mo experiment suggesting <0.1 μm of oxidative corrosion per year. Metallography, scanning electron microscopy (SEM), scanning transmission electron microscopy (TEM)/SEM evaluation of selected specimens gave no indication of active corrosion during the experiments. The TEM micrographs of ultra-thinned oxide on archive cladding and on

cladding from the 12-mo experiment are identical, suggesting very little corrosion activity, and again suggesting <0.1 μm of oxidative corrosion. No indication of localized corrosion was noted on either the cladding or the stainless steel wrap in areas of contact. The results suggest that the very slow oxidative corrosion predicted by extrapolation of higher temperature oxidation models to this lower temperature condition may be of the correct order of magnitude. If so, cladding corrosion is negligible (<1%) even for the long time periods under consideration (i.e., 10,000 yr). It is concluded that tests to actually measure corrosion under these conditions should make use of spent fuel cladding specimens with well-polished areas so that SEM evaluation can be used to identify localized corrosion, and Auger/ion milling techniques can be used to quantify the extremely thin oxidative corrosion films predicted by the oxidation models. Carbon-14 may be a very sensitive indicator of cladding-environment interaction once its distribution in the cladding has been accurately described.

II. INTRODUCTION

Spent nuclear fuel is one of the waste forms that is planned for placement in a nuclear waste repository. As such it must be completely characterized with respect to how it will respond to the various environments it will encounter during its first 10,000 yr of residence in the repository so that its performance in the repository can be modeled and appropriate engineered barriers can be designed. Spent fuel cladding is an integral part of the spent fuel and will, to a large extent, determine how the spent fuel behaves in time as a source of radionuclides that must be controlled by engineered barriers in the repository. The integrity of the cladding will, to a significant degree, control the environment that the spent fuel pellets experience in terms of oxidizing atmospheres and water. At the same time, the cladding integrity will strongly affect the transport of radionuclides away from the fuel via gaseous or fluid phase mechanisms. Oxidative corrosion of Zircaloy is the only probable mechanism that would seriously alter the cladding integrity as a result of exposure to the repository environment.[1] (The one exception might be oxidation of spent fuel in an already breached spent fuel rod causing the fuel to expand and disrupt the cladding.) For this reason, Lawrence Livermore National Laboratory (LLNL), as part of the Nevada Nuclear Waste Storage Investigations (NNWSI) Project, is sponsoring the Zircaloy Cladding Corrosion Degradation Study in progress at the Hanford Engineering Development Laboratory (HEDL). The NNWSI Project is investigating the suitability of the Topopah Spring Member of the Paintbrush Tuff at Yucca Mountain, Nevada, for potential siting of a high-level nuclear waste repository.

An evaluation of the projected history of the tuff repository identified two periods during which corrosion of the Zircaloy might occur, and even these conditions are so benign that they only rate consideration because of the hundreds or thousands of years that they may last.[2] Zircaloy cladding will be experimentally tested under the most severe conditions representative of these two environments. One experimental series will consist of exposing the cladding to ~120 psi, 170 °C water in an autoclave. In the other, Zircaloy

cladding will be exposed to 90 °C, tuff-equilibrated groundwater. Both electrochemical corrosion and stress corrosion cracking will be investigated in those environments.

To experimentally evaluate the various combinations of environments and corrosion mechanisms, six experimental tests are planned. The first two are scoping experiments designed to produce initial data and refine the experimental procedure. These are complete or now in progress. The results of these scoping experiments are expected to greatly improve the cost and time effectiveness of the principal experiments with respect to the amount and quality of data obtained.

The purpose of this report is to present the results of the electrochemical corrosion scoping experiment, which investigated the corrosion behavior of Zircaloy spent fuel cladding in hot (90 °C), tuff-equilibrated Well J-13 water.[3] Well J-13 water is believed to be a close approximation to the water that partially saturates the tuffs at the repository horizon.[4] The objective of this scoping experiment was to expose actual spent fuel cladding to a simulated tuff repository environment and to characterize the corrosion of the cladding in this environment. These results are compared to those summarized by Rothman[1] and the techniques employed in the work are evaluated with respect to their effectiveness in revealing corrosion effects.

III. EXPERIMENT DESIGN AND PROCEDURE

As has been described elsewhere,[1] the postclosure environment of a tuff repository will go through a hot period that will last about 1,000 yr during which the temperatures will be above the boiling point of water [(~95 °C) at the candidate repository horizon)]. Following that, temperatures will continue to slowly decrease, allowing groundwater to infiltrate the repository. If it is assumed that the spent fuel containers have breached by that time, spent fuel rods could be exposed to groundwater at a temperature around 90 °C.

Under these conditions, water will either seep or drip into the container through one or more breaches in the container. Barring the presence of a breach at the bottom of the container that would allow any water that entered to drain freely, water will eventually accumulate in the bottom of the container so that spent fuel rods will be partially covered with water. Water will also be drawn up along contact areas between rods and between rods and the container wall. Hence there will be opportunities for crevice corrosion, galvanic corrosion, and concentration-driven corrosion at water-air interfaces, as well as homogeneous corrosion.

The environment, along with the expected geometries of consolidated spent fuel in a container, was modeled for this experiment as realistically as possible in the following way. The breached container full of consolidated spent fuel was simulated by a small bundle of spent fuel cladding sections held together by a strip of reference repository container material. This assembly was maintained at 90 °C and partially submerged in a tuff-equilibrated groundwater from Well J-13. The expected crevices, contacts, materials interactions, and the temperature are reproduced in this experiment.

A. EQUIPMENT

The equipment for this experiment consisted of three silica jars with flared rims, ground flat, to facilitate sealing against Pyrex* plate glass lids. The cylindrical jar cavity was 54 mm by 152 mm. The lid had a glass handle epoxied at the center. A 16 mm diameter port was drilled through the lid so that its outer edge coincided with the inside wall of the jar. Teflon** stoppers were used to seal these ports.

During the experiment, the vessels were immersed in a hot bath which had an approximately 11 in. long by 5 in. wide by 6 in. deep stainless steel tank. The heat sensor was placed inside the tank on the bottom, and a 1/2 in.-high stainless steel platform in the tank provided a flat surface upon which to set the jars. The tank was filled with enough HTF-100*** oil-bath oil to come to within about 1 in. of the top of the tank when all of the jars were in place in the tank. Separate Type-K thermocouples were used to measure temperatures periodically in the oil bath and in the jar during the experiment. These were read out on the same digital thermometer.

Conductivity of the Well J-13 water was measured using a Beckman CEL-K1 conductivity probe which was inserted through the port in the Pyrex lid. This probe was modified by removing the bottom half of the glass enclosure around the platinum electrodes to facilitate removal of gas bubbles that tend to become trapped around the electrodes. The cell was used in conjunction with an Industrial Instruments RC-18 conductivity bridge.

B. EXPERIMENT MATERIALS AND PREPARATION

The cladding for these experiments was taken from Turkey Point spent fuel assembly B-17 which was discharged from service in 1975.[3] These particular rod sections were defueled and made alpha free by repeated ultrasonic cleaning

*Pyrex is a trademark of Pittsburgh Corning.
**Teflon is a trademark of E. I. duPont de Nemours & Company.
***HTF-100 is a trademark of Blue M Electric Co.

and 50% nitric acid washes (Ref. 5, p. 22). Note that zirconium has excellent corrosion resistance to nitric acid to concentrations of 90 wt% and temperatures of 200 °C.[6] The cladding selected for the experiments included material from different levels in the reactor core having thick and thin oxide films and a corresponding range of hydride inclusions.[7] By including cladding from various levels of the core, the different kinds of "crud" scale that develops on cladding should also be present in the experiment. This crud has a wide range of crystallinity and composition, from amorphous ferric oxides to crystalline iron, nickel, and chromium spinels.[8,9] Also, the thick oxide film is porous to a certain degree, adding more crevice-like environments in which extremes in solution chemistry may occur. The cladding sections (4.5 to 4.75 in. long) were plugged with Zircaloy-4 plugs machined from unirradiated rod material. The plugs were held in place with EPON* Resin 828 epoxy ("Z-cured" at 150 °C for 2 h).

As illustrated in Figure 1, the cladding sections were gathered into bundles of seven (six around one) and held in place with a 2 in. by 6 in. 304L SS strip and a 301 SS hose clamp (410 SS screw) (see Figure 2). The wrap was positioned so that it would be intersected by the water surface during the experiments. Table 1 specifically indicates the makeup of each bundle. This configuration simulates all of the geometries and materials contacts in conjunction with exposure to all of the air and water combinations expected in the repository situation.

Crushed tuff (<2 mm) placed around the bundle ~1 in. deep came from a surface outcrop of the Topopah Spring member of the tuff sequence near the repository site. The crushed tuff was first washed in Well J-13 water at ~25 °C for about 1 h and then again at 90 °C overnight. Washing consisted of placing ~200 g of crushed tuff in ~900 mL of the well water, agitating, and then allowing the system to settle and decanting off the cleared fluid. Following hot water washing, the water-tuff mixture was separated by filtering. The wet tuff was then dried in a muffle furnace overnight

*EPON is a trademark of the Shell Chemical Company.

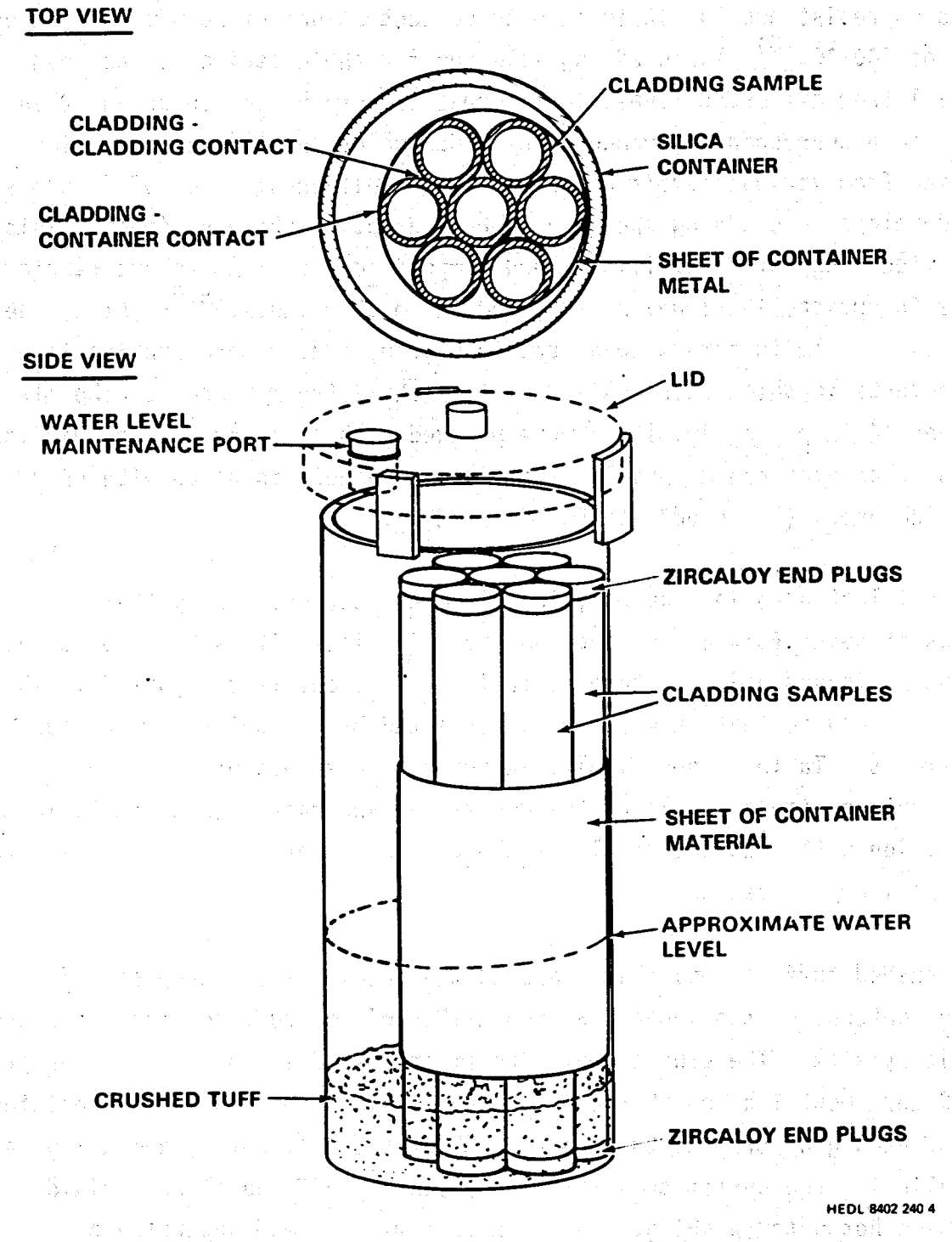

FIGURE 1. Schematic of the Silica Jar with Cladding Bundle, Water, and Crushed Tuff in Place.

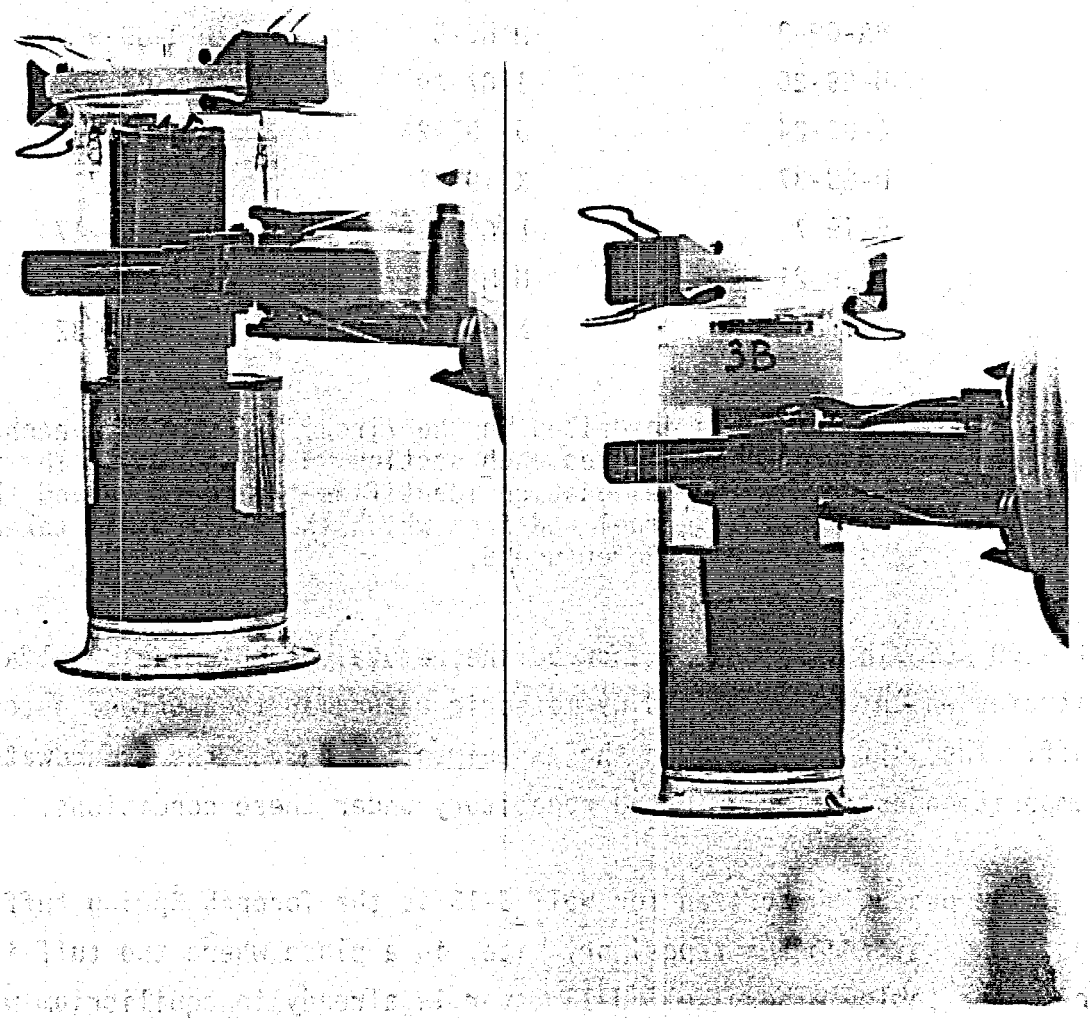

FIGURE 2. Jars 1 and 3 Containing TP-B17-ECS-AA and TP-B17-ECS-CC Just Before Placing Them Into the Oil Bath.

TABLE 1

TURKEY POINT[5] DEFUELED CLADDING SECTIONS
MAKING UP ELECTROCHEMICAL CORROSION SCOPING EXPERIMENT BUNDLES

TP-B17-ECS-AA	TP-B17-ECS-BB	TP-B17-ECS-CC
*A-G9-3	H-H6-5	O-G9-9
B-G9-20	I-G7-19	P-H6-3
C-G9-24	J- G7-24	Q-H6-17
D-G9-37	K-I9-27	R-J8-7
E-I9-7	L-G9-7	S-J8- 17
F-I9-21	M-H6-21	T-J8-21
G-I9-32	N-H6-32	U-J8- 32

*This letter is inscribed on the Zircaloy-4 plugs in each section and identifies each section in the bundle. The rest of the section designation identifies the fuel rod and the position in the fuel rod from which the section was taken, as described in Reference 5.

at ~100 °C. This procedure assured the removal of chlorides, sulfates, and nitrates which are deposited by meteoric waters in the surface outcrop of the tuff. The tuff is placed in the experiment to buffer the groundwater composition as it would in the repository under these conditions.

The producing horizon for Well J-13 is the Topopah Spring tuff in a location away from the repository site, in a place where the tuff is below the water table. Thus, Well J-13 water is already in equilibrium with tuff at ambient temperature. The presence of tuff in the experiment allows it to re-equilibrate with tuff at 90 °C and remain close to equilibrium in spite of the mineral deposition that occurred during the experiment [i.e., the "white ppt" which is discussed later (see Table 2)]. The Well J-13 water came from a 55-gal barrel ("F") supplied by LLNL to HEDL in 1983. An analysis of this water is given in Table 2.

TABLE 2

WELL J-13 WATER ANALYSIS DURING AND AT THE END OF EACH EXPERIMENT

	TP-B17-ECS-BB 9/7/84(1)	TP-B17-ECS-AA 11/15/84	P-B17-ECS-CC 11/15/84	TP-B17-ECS-CC 1/8/85(1)	TP-B17-ECS-AA 6/27/85(1)	J-13 Prior to Startup of Exp	White Precipitate
Al	0.86	0.115	0.075	0.15	0.15	0.11	0.02(3)
Ca	8.50	9.202	10.80	9.92	10.4	15.0	8.00
Co	<0.013	<0.01	<0.01	0.02	<0.01	(Cr)<0.0	(Cr)0.009
Fe	0.12	<0.01	<0.01	<0.01	<0.01	<0.01	0.01
K	8.90	7.868	8.896	4.56	5.19	5.53	0.09
Mg	<0.25	<0.25	<0.25	<0.25	<0.25	2.10	ND
Mn	0.006	<0.005	<0.005	<0.005	<0.005	--	0.03
Na	48.3	35.29	45.18	31.3	27.3	49.5	0.02
Ni	0.029	<0.020	<0.020	<0.02	<0.02	--	ND
Si	64.4	62.97	58.90	49.4	43.4	31.9	60.0
Zr	<0.01	0.015	0.013	<0.01	<0.01	--	ND
F-(2)	4.3	2.71	5.1	2.3	2.0	2.7	ND
Cl-	8.4	5.30	6.84	5.2	6.3	7.3	0.03
NO3	6.4	1.5	2.0	1.7	1.6(NO2-1.8)	8.7	(O)10.0
SO4	30.2	14.5	25.7	16.0	12.3	18.8	(S)0.02
(CO3)	5.6	10.6	9.0	3.0	7.0	16.8	(C)20.0
Reported as inorganic C				(All C)			

(1) Analyzed at termination of 2-, 6-, and 12-month experiments, respectively. Analyses ppm.
(2) Organic anions will interfere with F- analyses.
(3) Spectrographic analysis given in elemental % (semiquantitative-correct to a factor of 3).

C. EXPERIMENT PROCEDURE

The experiments were assembled by first loading 1 to 1 1/4 in. of moistened (Well J-13 water) crushed tuff into the jars, then setting the bundles in place into the tuff. The lip around the top of each jar was given a very thin coat of high-temperature vacuum grease, and then the lids were put in place and held tightly by clamps. Enough Well J-13 water was then added to bring the water line about halfway up on the side of each cladding bundle and a reference mark made so that water level changes could be determined. Next the loaded jars were placed into the oil bath, the power turned on, and the experiments were allowed to warm up with access ports open. As soon as the water temperatures reached ~85 °C, the access ports were plugged with Teflon* stoppers.

While the experiments were running, the water level, temperature, and chemistry were monitored. The water level and temperature were monitored to make sure that the corrosion environment would remain constant during the course of the experiments, while the water chemistry was monitored so that any changes that might suggest the onset of rapid corrosion or other disturbance in the experiment system would be detected close to the time it actually occurred.

The water levels were maintained within 0.0625 in. (i.e., ~3 mL) of the original fill level at least two-thirds of the time for the 2-, 6-, and 12-mo experiments (see Table 3). Periods of water loss generally occurred after a given experiment had been open to make a temperature determination, etc. Apparently the Teflon plug did not seat perfectly each time, resulting in periods of water loss. The water levels were more than 1/4 in. low <5% of the duration of the experiment and, as discussed below, there was no measured effect on the chemistry of any of the experiments due to the variation of the water level.

---

*Teflon is a trademark of E. I. duPont de Nemours & Company.

TABLE 3

TEMPERATURE, pH, AND SOLUTION CONDUCTIVITY

Experiment	Water Level Maintenance[a]	Temperature	pH	Conductivity (μS)
2 Mo	73%	89.9 ± 1.1 °C[b]	8.76 ± .11	754.0 ± 83.0
6 Mo	67%	89.2 ± 0.9 °C	8.68 ± .21	--
12 Mo	66%	89.1 ± 1.7 °C	8.59 ± .30	724.0 ± 106.0

[a]Percent of time at original fill level.
[b]One standard deviation.

The target temperature for each experiment was 90 °C. Through initial benchtop experiments it was found that the oil bath needed to be maintained at 100 to 101 °C to keep the water in the jar at 90 ±1 °C with the oil 1 in. above the water line in the jar. The temperature control achieved is shown in Table 3. For the longer experiments, it was necessary to periodically increase the power setting on the oil bath to maintain the experiment temperature. This was apparently necessary because of a slight breakdown of the oil used in the oil bath forming a dark colored oil with modified heat transfer characteristics.

Both pH and conductivity (first 140 d) were routinely determined for each experiment. The pH was determined on a small aliquot removed from the jar. This was done at weekly intervals during the first 2 wk of the experiment and then at 2 wk intervals until the experiment was terminated. By the time the first determination was made, the pH was already in the value range indicated in Table 3 and the trend remained flat for the duration of each experiment. Similarly, the conductivity appeared to remain constant over the period it was measured. The conductivity was measured in situ by inserting the probe through the port in the lid. The measurement was difficult to make because the cell could not be seen in the jar during the measurement and

because of limited room to insert the probe. (The measurements were suspended when the bundle in the 12-mo experiment shifted enough to interfere with the insertion of the conductivity probe.) These difficulties are believed to account for the amount of scatter observed in the data (Table 3) and obscure any small trends that might be present.

The elemental solute chemistry of the solutions in contact with the cladding bundles is shown in Table 2 along with the analysis of the Well J-13 water prior to startup and a semiquantitative spectrographic analysis of the white precipitate (see Figure 3) that formed on the cladding bundles during the experiments. The Well J-13 water from each experiment was analyzed at the termination of each experiment. Intermediate analyses were performed on the 6- and 12-mo experiments. Any time water was physically removed from the experiments it was replaced volume for volume with Well J-13 water. Losses believed to be due to evaporation were replaced with deionized water. As will be discussed later, it appears that the formation of the white precipitate explains most of the shifts in the water chemistry that cannot be attributed to equilibration (or interaction) with the crushed tuff and/or silica jar.

The carbon in the Well J-13 water was determined more frequently and in more detail. The results for inorganic, organic, and carbon-14 are reported in Table 4. Organic carbon was of primary importance because of its potential as a passivating agent and the fact that the epoxy used to seal the end of the cladding sections may act as a source of organic carbon, particularly in the presence of a radiation field. At the midpoint of the 12-mo experiment, the Well J-13 water was changed out twice to see if that would significantly change the observed level of organic carbon. This was done on the 191st d of the 12-mo experiment. At that time the water was withdrawn down to the level of the crushed tuff and refilled with fresh Well J-13 water. It was then allowed to stand for ~24 h (at 90 °C), and the process was repeated. Subsequent analyses were made as indicated in Table 4. Carbon-14 measurements were included late in the experiment after both the 2-mo and 6-mo experiments had been terminated, but measurements were made on the Well J-13 water taken from those experiments. These values suggest that carbon-14 is being released from

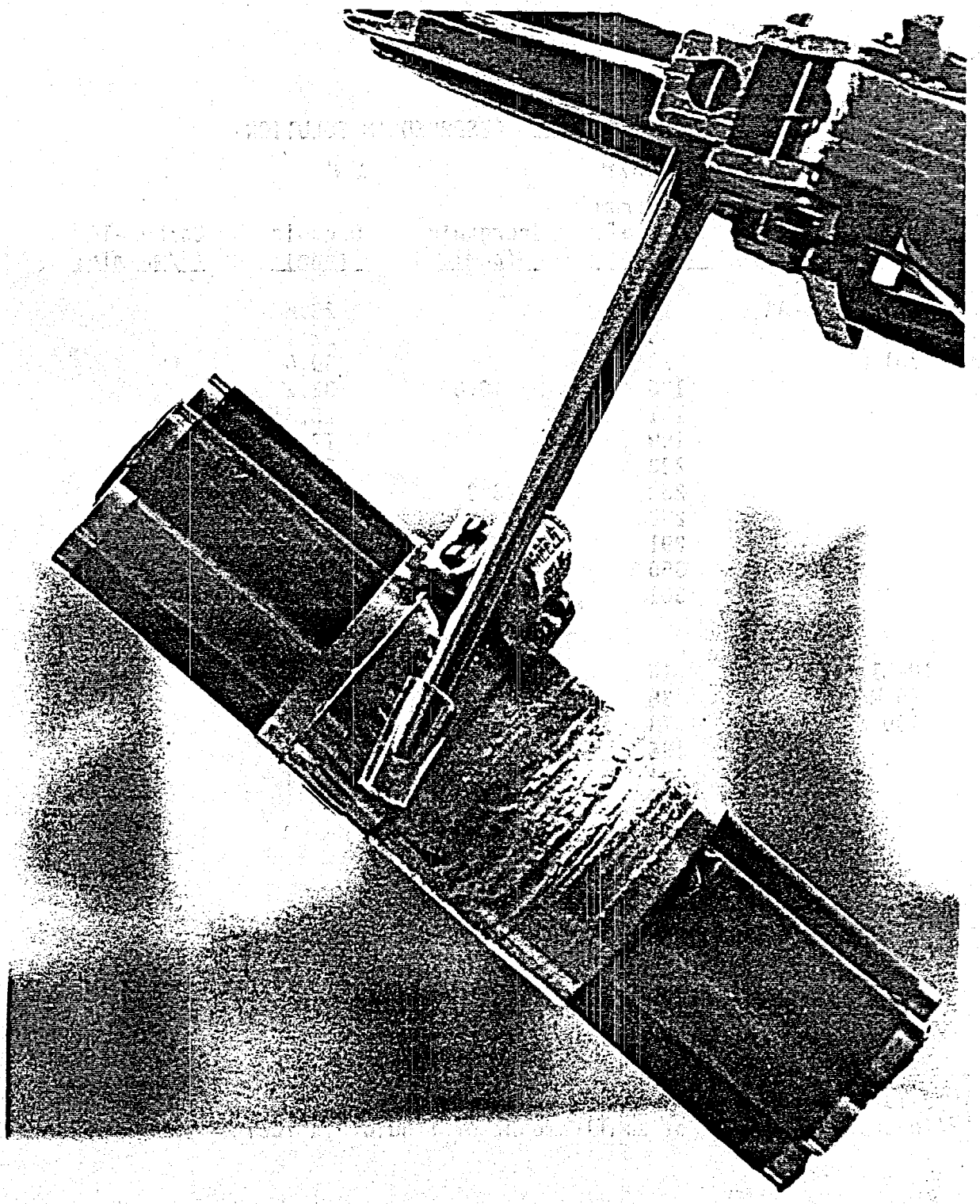

38808140.2

FIGURE 3. Zircaloy-4 Cladding Bundle Just Removed from Jar. (White deposit on 304L SS wrap formed at the water line. It is believed to consist principally of silica and calcium carbonate. TP-B17-ECS-CC the 6-mo experiment.)

TABLE 4

CARBON SPECIES OBSERVED IN SOLUTION

Experiment	Days from Start of Run	Inorganic (ppm)	Organic (ppm)	Carbon-14 (d/mL-min)
TP-B17-ECS-AA	16		28.6	
(12 Mo)	38		22.9	
361 D	73		39.0	
	136	10.6	32.2	
	191		25.3*	
	199		12.0	
	220		20.8	
	262	6.9	24.4	
	288			165
	291	5.7	24.1	
	360	6.9	24.8	
	361			180
TP-B17-ECS-CC	16		34.1	
(6 Mo)	38		38.0	
190 D	73		49.0	
	136	9.0	47.7	
	191	3.0	37.4	
	295			124
	361			110
TP-B17-ECS-BB	20		28.8	
(2 Mo)	42		26.0	
70 D	77	5.6		
	306			52
	365			13[b]

[a] J-13 completely exchanges for fresh J-13 at this time.
[b] Inaccurate because of small amount of liquid available.

the cladding surface. The decreasing values in the 2- and 6-mo experiment solutions indicate loss of carbon-14 to the environment (i.e., container surfaces, atmosphere, etc.). Carbon-14 is discussed in more detail at the end of this report.

IV. POSTEXPERIMENT EVALUATION OF THE SPENT FUEL CLADDING

After each experiment was terminated, the bundle of spent fuel cladding sections was lifted out of the silica jar and visually inspected. After it had been allowed to dry it was documented photographically from several angles and then disassembled. Prior to disassembly, several small fiducial marks were made both on the end caps and on the cladding to maintain knowledge of spatial relationships after the bundle had been taken apart. After disassembly, each part was photographed separately. Based on a visual examination, two cladding sections (one with a thick oxide film and one with a thin oxide film) were chosen for detailed examination via metallography, SEM and, in a few cases, scanning TEM with TEM and electron diffraction analyses at higher magnifications.

A. GENERAL OBSERVATIONS

Macroscopically, little appears to have happened to either the Zircaloy cladding or the 304L SS wrap during these experiments. The 6-mo experiment shown in Figure 4 just after removal from the oil bath is typical of the 2-, 6-, and 12-mo experiments. The cladding bundle from the 6-mo experiment is shown in Figure 3 and is also typical of those from the other experiments. The white deposit on the stainless wrap corresponds to the water level in the jar during the experiment. Once the white deposit was dry, it was easily scraped off of the stainless steel. As well as can be determined, the white precipitate is deposited from the water at the water-air interface and does not contain any corrosion products (Table 2). The appearance of the cladding and the Zircaloy-4 end plugs above and below the water line is the same (see Figure 3). Again this was true for the 2-, 6-, and 12-mo experiments. The dark deposits on the ends of the Zircaloy plugs is excess epoxy which has been darkened by the radiation environment. Figure 5 shows how the cladding bundle stood down in the crushed tuff in the bottom of the jar. In Figure 6 there is a thin, black wavy line (indicated by the arrow) about 1 in. from the bottom that might coincide with the top of the crushed tuff. The cladding itself appears exactly the same above and below this line. This line looks

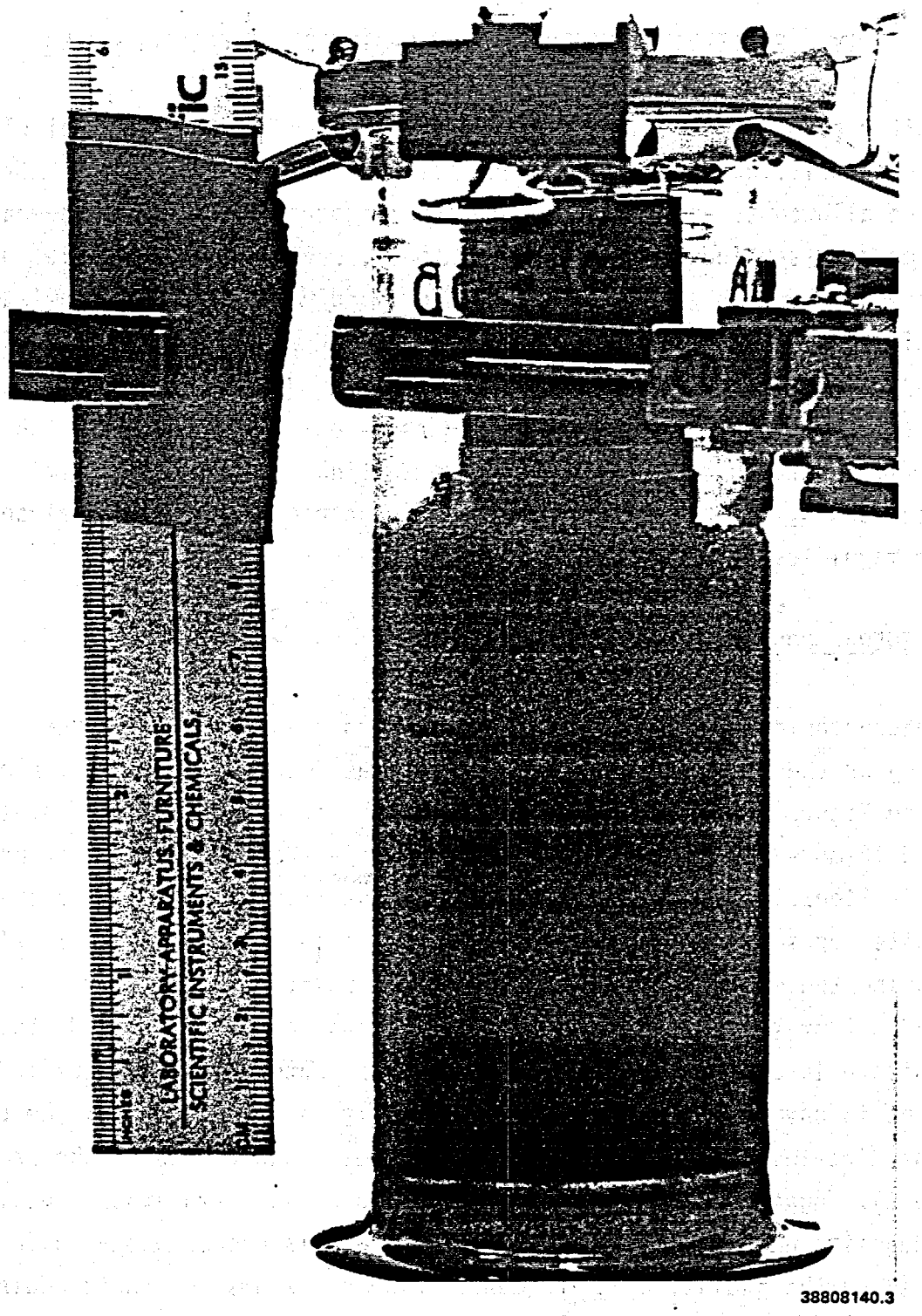

FIGURE 4. Six-Month Experiment Just Removed from the Hot Oil Bath. (Jar appears dark where it contacted the oil because of a deposit from the oil on its surface. Water line just visible ~1 in. below top of darkened region. TP-B17-ECS-CC - the 6-mo experiment.)

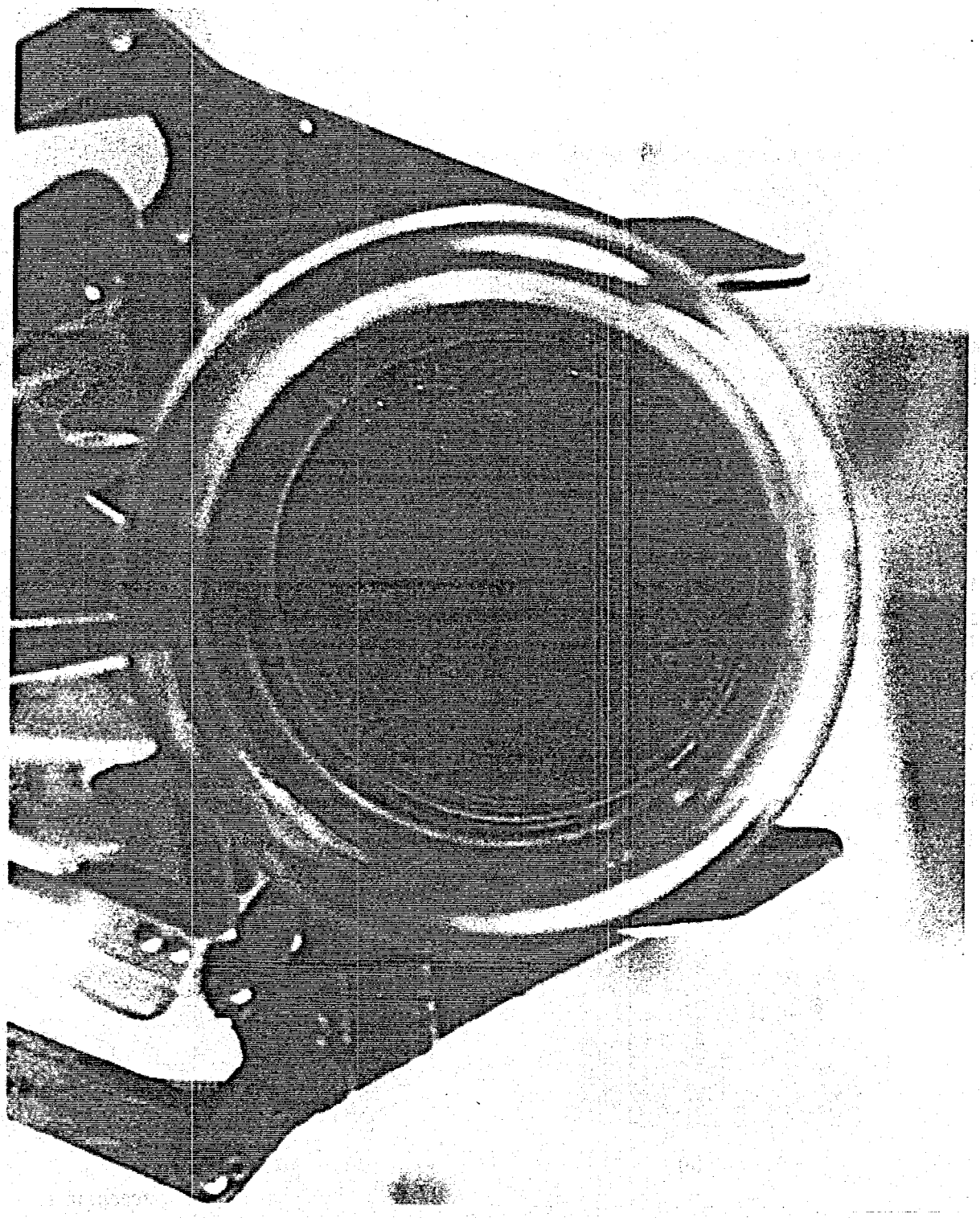

38808140.4

FIGURE 5. Crushed Tuff in the Bottom of the Jar (Figure 1). (Cladding bundle sat in the hole in the tuff. This is from the 6-mo experiment.)

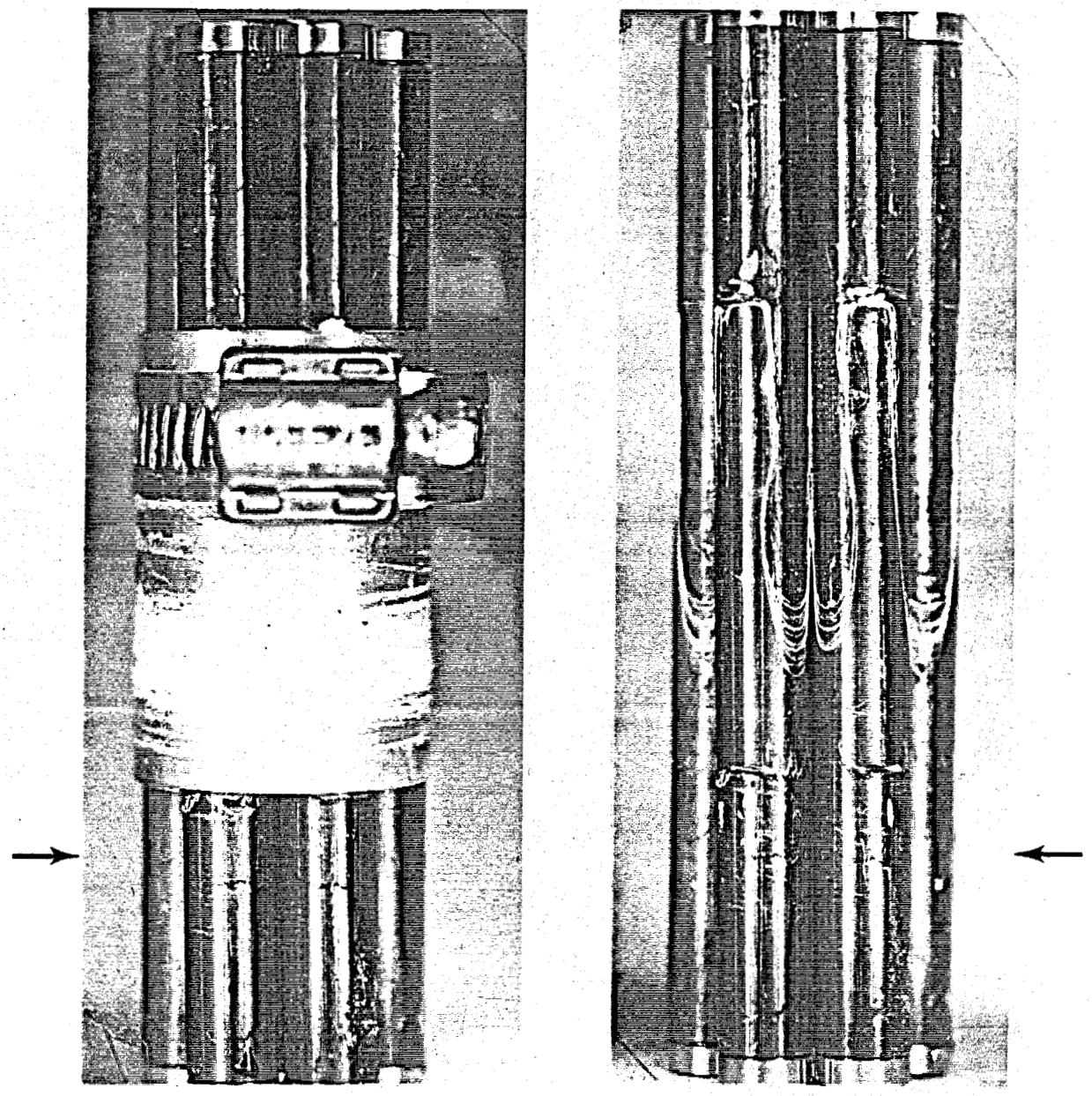

FIGURE 6. Cladding Bundle from 6-Month Experiment (Figures 4 and 5) before (a) and after (b) Removal of the 304L SS Wrap. Small cuts on cladding in (b) are fiducial marks. Arrows mark the location of the "wavy line" produced at the water-tuff interface.

very similar to markings observed near the water-air interface and is probably due to the same physical phenomenon. These areas were analyzed in more detail via metallography and SEM and the results are discussed in Section IV of this report. When the wrap is removed, as shown in Figure 6b, the white deposits indicating the water-air interface against the cladding show that capillary forces redistributed the water inside the wrap. The water was drawn to the top of the wrap and to an undetermined height between the cladding sections. Again, little, if any, effect could be observed other than what appeared to be interference fringes (black lines) in some areas where the 304L SS and Zircaloy cladding were in close proximity (see Figure 6b, the area inside the white deposit line near the top of where the wrap was located).

Another indication that very little oxidative corrosion has occurred was observed in regions where the oxide was transforming from the thinner pretransition oxide film to the gray posttransition oxide film. In these areas the gray oxide forms patches that coalesce eventually but at an intermediate stage the patches are separated by thin lines and triangular patches of black pretransition oxide. In the 6-mo experiment, one section of spent fuel had a particularly well-developed pattern that did not perceptibly change during the course of the experiment. The oxide film changes from a minimum [(~2 μm) at the bottom)] to a maximum (~20 μm) thickness over a distance of about 2,500 mm whereas the transition from pretransition to posttransition oxide occurred over a distance of 50 mm, or ~0.4 μm thickness change. Since absolutely no change in the gray-black pattern was observed, change in thickness of the oxide film must have been much <0.4 μm.

Figure 7 shows the inside surface of the 304L SS wrap. These are from the 12-mo and 2-mo experiments, but those from the 6-mo experiment appeared to be exactly the same as the 2-mo wrap. The only features suggesting any interaction are the dark vertical lines that coincide with the line of contact between the wrap and the cladding sections, but these did not appear to change with time. As shown in Figure 7, they are probably the result of abrasion of the pickled surface of the stainless steel wrap which occurred during the assembly of the bundle of cladding sections.

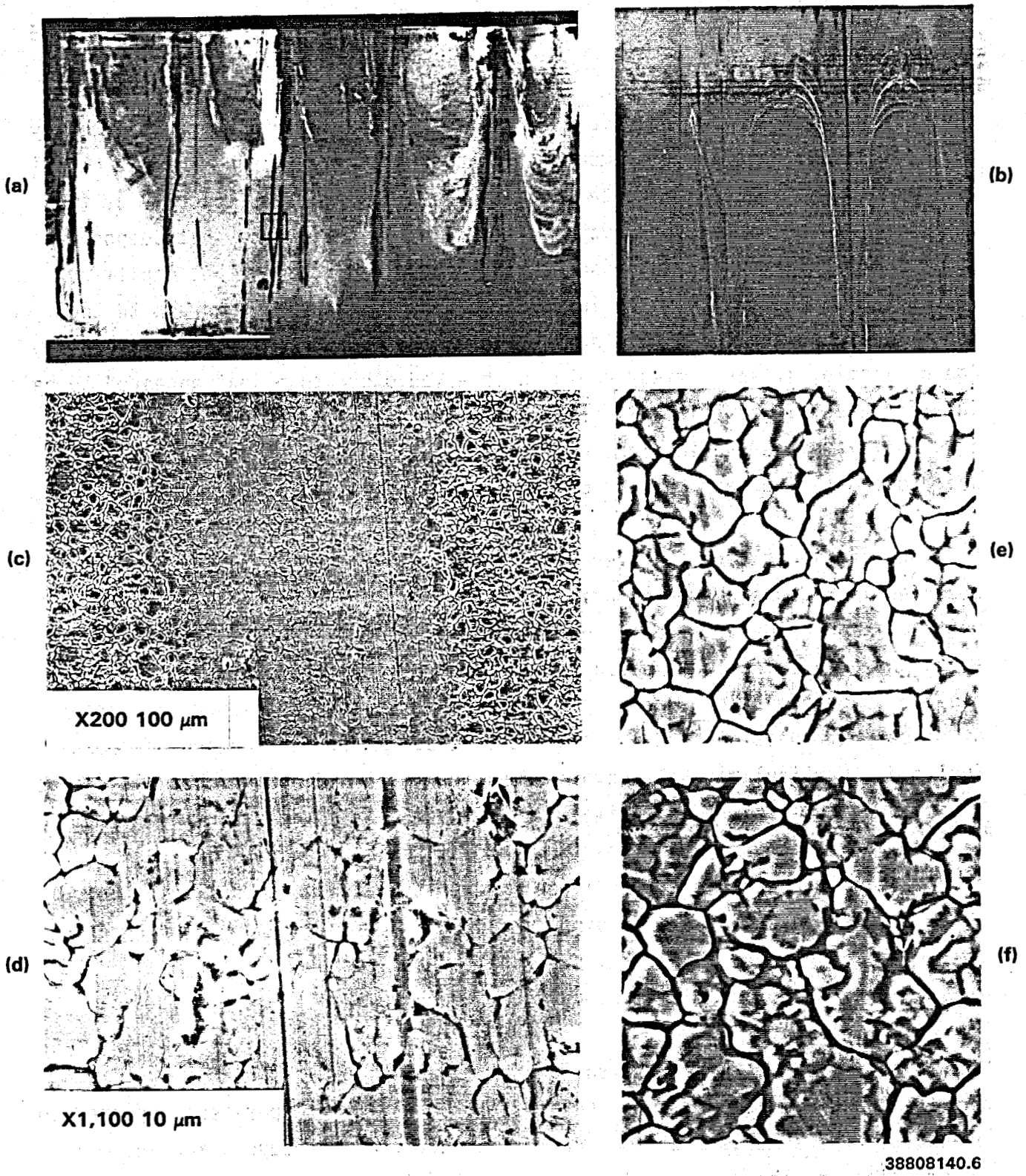

FIGURE 7. Inside Surface of 304L SS Wrap (2 in. high) from the 12-mo (a) and the 2-mo (b) Experiments (6-mo looks the same). [The dark vertical lines in (a) and (b) coincide with the lines of contact with the cladding sections. White deposit indicates the water line during the experiment. Under magnification the dark area in (a) (rectangle) is shown to be a smoothed area, (c) and (d). Unabraded surfaces appear completely unaffected by the experiment, compare (e) with (f) an archive specimen. Note (d), (e), and (f) have the same scale.]

In conclusion, there is no visible macroscopic evidence that the Zircaloy spent fuel cladding has reacted in any measurable way with the environment produced by tuff equilibrated Well J-13 water and 304L SS.

B. POSTEXPERIMENT CLADDING SAMPLE SELECTION AND PREPARATION

These electrochemical corrosion experiments were set up to explore the potential corrosion conditions that might occur under tuff repository conditions after about 1,000 yr. As such, the experiment bundles were constructed to simulate consolidated spent fuel rods in a 304L SS container exposed to infiltrating ground water. Corrosion environments generated included air/water interfaces, crevices, dissimilar metal contacts, thick water films, etc. Available evidence, e.g., Rothman[1], indicated that little, if any, easily discernible corrosion was likely to occur. Therefore, since it is not possible to characterize a specimen microscopically prior to the experiment, it was necessary to choose samples on which areas of localized corrosion could possibly be recognized by comparing them to adjacent areas that had been less affected by corrosion in the experimental environment. Hence, samples were taken so that they extended across areas where localized corrosion might have occurred, such as dissimilar metal contacts, areas where crevices would be formed, water-air interfaces, etc. The samples were taken according to the scheme illustrated in Figure 8 and they include material exposed to all of those environments.

Three levels were sampled, as shown in Figure 8, by cutting 1/8-in. rings out of the fuel rod section. The upper ring was exposed to both high humidity air and water during the course of the experiment because even though it is above the water level in the jar during the experiment, water is drawn up along the wrap-cladding and cladding-cladding lines of contact by capillary action (see Figure 7). These sections, therefore, include several water-air interfaces. The middle ring was taken at a level close to the water line as seen from the outside of the spent fuel bundle and in contact with the 304L SS wrap. The middle ring sample may include several air-water interfaces (if the static water level fell below the sampling level) and the lines of contact

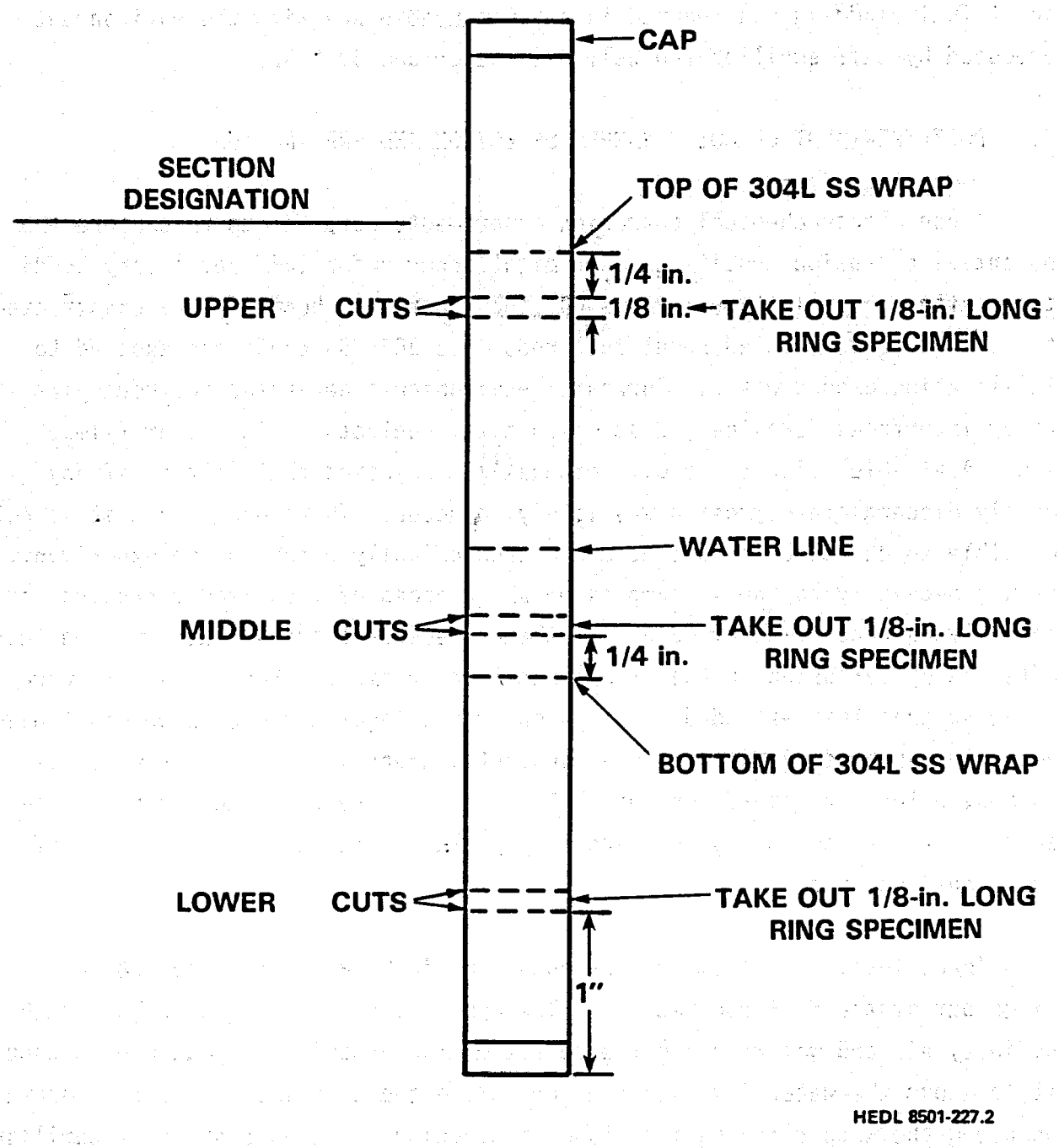

FIGURE 8. Sectioning Diagram for Cladding Section. (Each 1/8 in.-ring section samples all micro-environments present at the particular level. The three levels include: air/water interfaces, cladding/cladding and cladding/wrap contact lines, and the proximity of crushed tuff.)

between the cladding sections and the line of contact with the 304L wrap, all of which were effectively under water. The lower ring was taken at a level at which it was exposed directly to the water just above the crushed tuff. This sample is representative of material exposed to bulk water conditions in contrast to the middle and upper specimens, where various materials contacts were present. The rest of the spent fuel rod section was stored for future work if the evidence warranted more extensive sample evaluation. Areas in contact with the tuff were not included because they appeared macroscopically exactly the same as higher areas which were in contact with just the water. The thin dark line observed on some spent fuel sections, as already mentioned, appeared to be the same but less intense as markings associated with crevice areas beneath the wrap. Hence, the upper and middle specimen rings included this kind of phenomenon. These three samples should display the effects of corrosion at some position if detectable corrosion occurred during this experiment.

The sampling pattern applied to material from the 2-mo experiment differed from that shown in Figure 8 in that it did not include material from the area near the bottom of the wrap. Also, the polished metallographic specimens used for both optical and scanning electron microscope evaluation were cut at a low angle to the oxide surface to exaggerate the thickness of the oxide film and the features of the oxide-metal interface. However, these polished sections were difficult to prepare and did not result in significant additional information so subsequent samples were cut and polished at right angles to the oxide surface.

Samples for TEM/SEM evaluation were taken from areas adjacent to the metallographic specimens indicated in Figure 8. From these ion milled, ultrathin (to transmit the electron beam) sections are produced. The disadvantage in this case is that only a small fraction of the cladding surface can be surveyed in a given sample and they are difficult and expensive to produce. Specimens were only produced from the 12-mo experiment in which any corrosion effects should be most advanced. One set came from beneath the wrap and another from above the wrap out of the Well J-13 water.

Two cladding segments from each of the 2-mo, 6-mo, and 12-mo experiments were chosen for sampling. One had the characteristic gray appearance of a "posttransition" oxide film and the other was black, characteristic of a pretransition oxide film. The difference between these films is their thickness and internal texture. They are representative of the two types of films found on PWR spent fuel rods. These two types of oxide film are shown in Figure 9.

C. POSTEXPERIMENT CLADDING METALLOGRAPHY

All of the polished sections were viewed on a Bausch and Lomb reflected light microscope remotized for use in a hot cell. It gave a good flat image at 750X. Hence, this magnification was used for surveying each polished section visually. Photograph micros were made of selected areas at 75X or 100X and 750X.

In general, all of the observations can be summarized by the photographs shown in Figure 9. After evaluating sets of polished sections from the 2-mo, 6-mo, and 12-mo tests, no effect of the experiment could be identified in the polished sections at a magnification of 750X. The sections shown in Figure 9 while taken from the upper area could be from any area in the experimental environment: metal/metal contacts, at the air/water contact, in air, submerged in Well J-13 water, near the tuff, etc. More pertinent, there was no corrosion evident at this scale with either general category oxide film. Thick or thin, they both appear to be inert to the repository environment simulated in this experiment.

Figures 10 and 11 show a more extensive set of cladding specimens from the 6-mo experiment. An archive specimen mounted with each experiment specimen allows the artifacts of polishing to be taken into account when evaluating them. Overall the oxide films from the experimental specimens are identical in appearance to those on cladding that was never exposed to the experiment environment. The rough (scalloped) appearance that increases in amplitude with increasing oxide thickness was observed in all sections of both Turkey Point and H. B. Robinson cladding material that the author was able

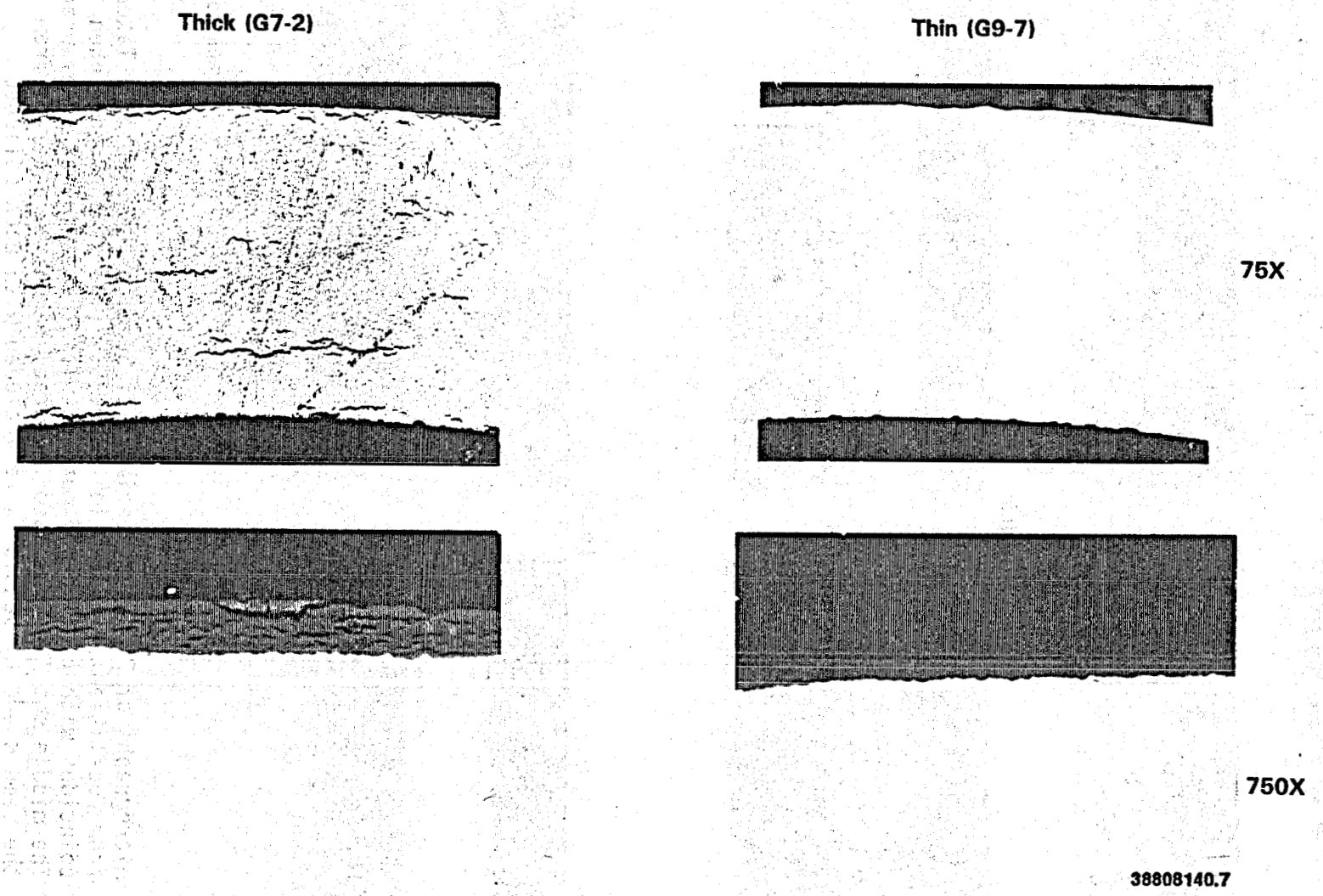

FIGURE 9. Representative Metallographic Sections from the 2-mo Experiment (a) Black thin pretransition oxide without porosity, (b) Gray" thick posttransition oxide with porosity. No difference was observed between contact (cladding-cladding or cladding-SS wrap) and noncontact areas. (This was true above and below the water line as well as at the water line.)

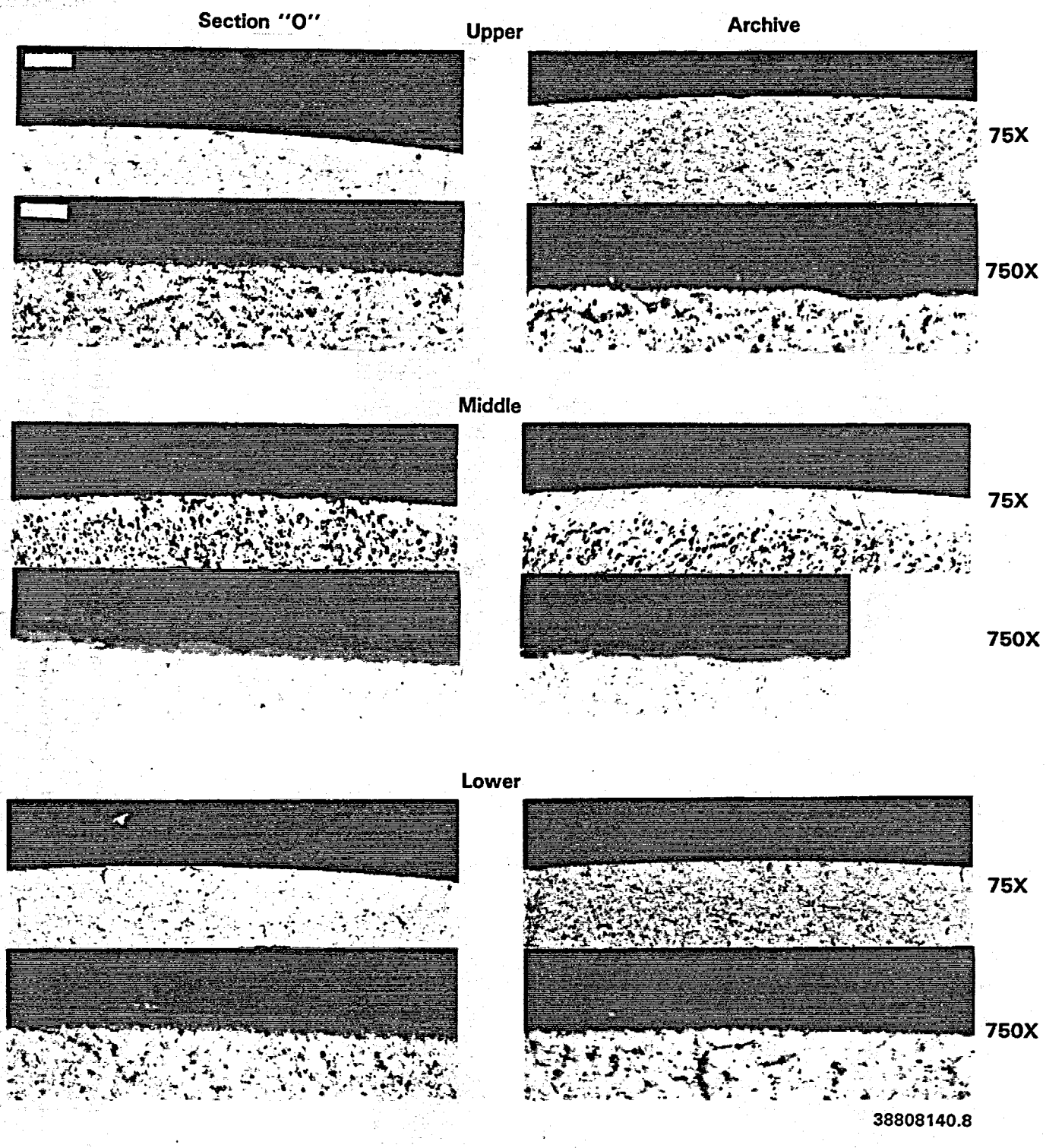

FIGURE 10. Micrographs of Polished Specimens of Section "O" (Table 1) Taken from Localities Indicated in Figure 8. (The area photographed coincides with the line of contact with the stainless steel wrap. The middle section contacted the wrap. Archive specimens from the same cladding section were included with each polished specimen for purposes of comparison (6-mo experiment). White bars on upper left micrographs equal 100 and 10 μm, respectively.)

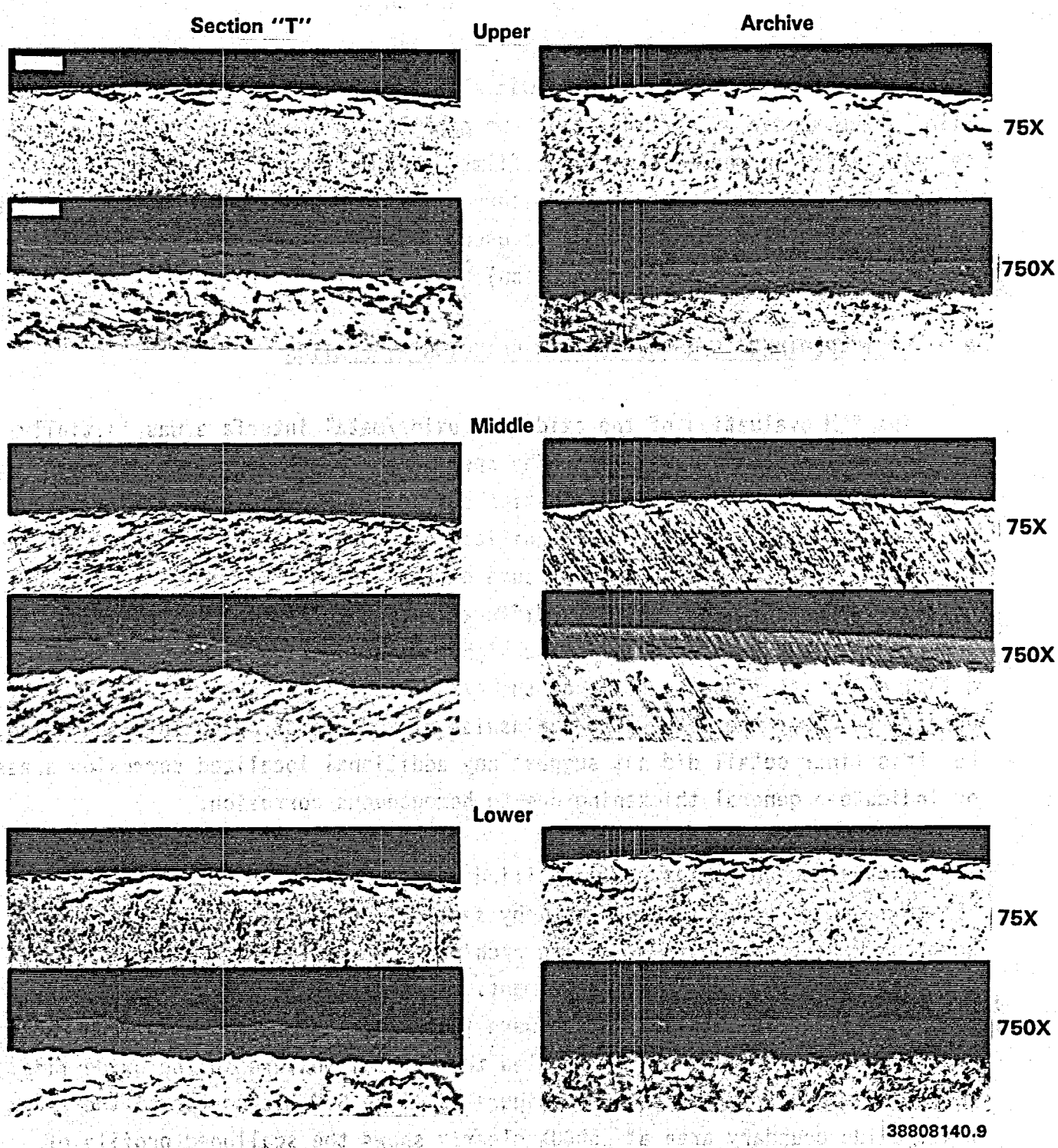

FIGURE 11. Micrographs of Polished Specimens of Section "T" (Table 1). (See Figure 10. Dark inclusions in 75X micrographs are hydrides. Scale bars on upper left micrographs equal 100 and 10 μm, respectively.)

to evaluate microscopically. This was also true of the porosity of the oxide film, which appear as partings that run parallel to the metal-oxide interface between layers in the thicker oxide films. Any differences between specimens exposed to the simulated tuff repository conditions and those not exposed were below the resolving power of the microscope (i.e., on the order of several tenths of a μm for localized corrosion).

D. POSTEXPERIMENT SEM AND SEM/TEM CLADDING EVALUATION

The SEM evaluation of the oxide and oxide/metal interface was initially carried out on polished metallography specimens from the 2-mo experiment. The SEM did give a higher magnification but, due to specimen radioactivity, the amount of additional useful magnification was only about a factor of three (i.e., to 2000X). Figure 12 shows some of the typical SEM micrographs obtained. Again in this case, no differences were detectable between any of the areas in the 2-mo material. The higher magnification did reveal more detail of the scalloped profile of the oxide/metal interface. The oxide appears to embay the metal with peninsulas of metal protruding into the oxide, but this finer detail did not suggest any additional localized corrosion areas or indicate a general thickening due to homogeneous corrosion.

Because no corrosion was identified at the resolution obtained using the SEM on standard polished metallography sections, ion milled ultra-thin sections were prepared from sibling archive material (I9-27 Turkey Point) and from material from the 12-mo experiment. In addition to evaluation at very good SEM resolution, these samples were further thinned via ion milling and viewed in the TEM mode, which revealed the crystal texture in the oxide film. This archive material is shown in Figure 13. The SEM micrograph of the metal/oxide boundary area at 15000X clearly shows the scalloped profile of the metal/oxide interface. In this particular section a band of metal milled differently than the bulk of the metal and might represent an oxygen-saturated layer of metal. Even at this higher magnification the metal/oxide boundary shows no tendency to part. Several examples of TEM micrographs, some with associated electron diffraction patterns, are also shown in Figure 13. The

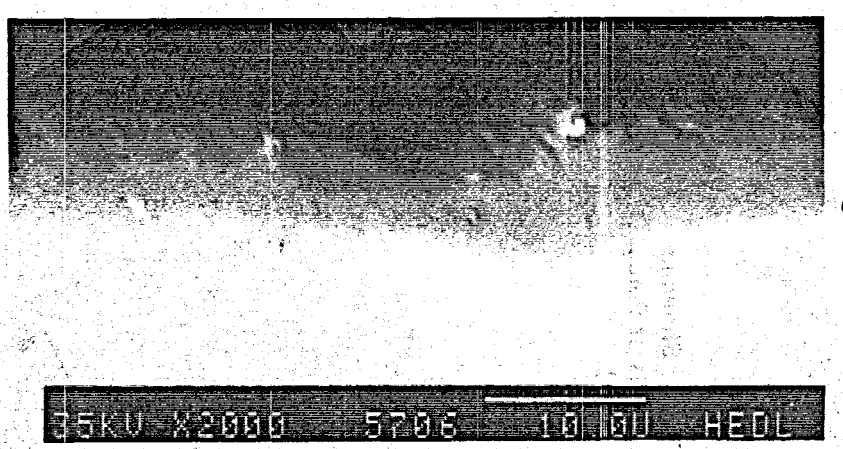

FIGURE 12. SEM Micrographs of Polished Sections of Cladding from the 2-Mo Experiment. (a,b) "Black" thin, pretransition oxide without porosity; (c) "Gray" thick posttransition oxide with porosity. Both have the same wavy or scalloped metal/oxide boundary shown in Figure 13. High radiation makes it difficult to get the same quality of image as shown in Figure 13. (Note these sections were polished at a low angle to the surface, exaggerating the oxide thickness and the texture of the oxide/metal interface.)

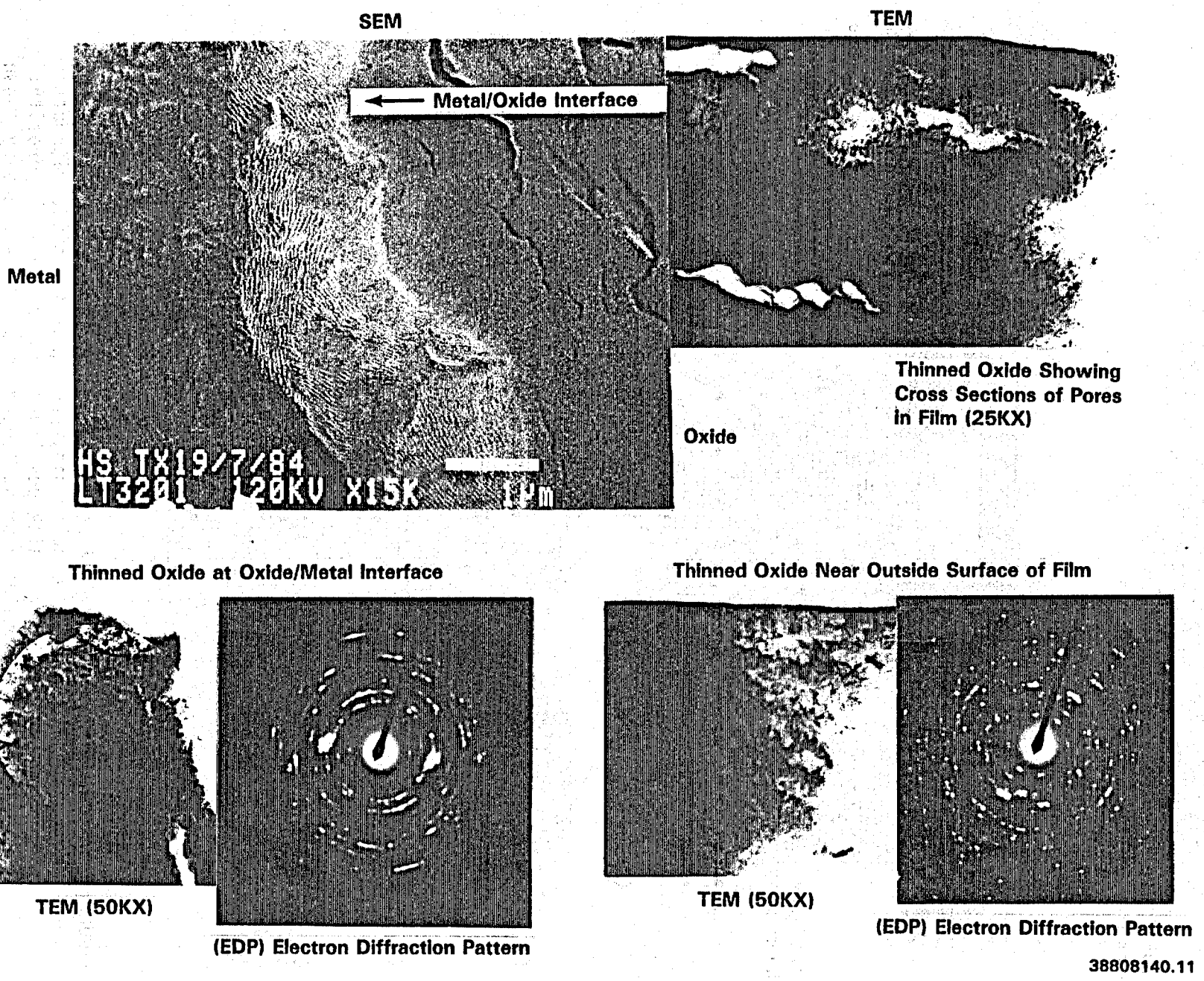

FIGURE 13. Scanning Electron Microscopy and Transmission Electron Microscopy Micrographs of a Transverse Section of the Oxide Film on Turkey Point Spent Fuel Cladding Archive Specimen with Associated Electron Diffraction Patterns (light circle on TEM image indicates area that generated the diffraction pattern. EDP suggests a finer-grained oxide next to oxide/metal interface and that monoclinic zirconia is the main phase at both levels.)

film is made up of distinct grains of ZrO_2 on the order of ~400 Å in diameter. The porosity (50KX TEM, left side of Figure 13) appears to be bounded by a nonporous boundary of grains. The electron diffraction patterns indicate the crystal structure was monoclinic zirconia[10,11] and the crystallite size increased with distance from the interface.

Based on the success with the archive sample, it was decided to employ the same techniques on specimens from the 12-mo experiment because cladding material from this experiment should exhibit the effects of corrosion if any are going to be found. Two specimens from Section E and two specimens from Section D were taken from the area along the line of contact with the stainless steel wrap just beneath the water line and from near the top of the cladding sections. However, only the specimen from Section E below the water line ion milled well enough to be directly compared with the archive material.

Some typical SEM micrographs are shown in Figure 14. There were differences in the way this specimen milled as compared to the archive specimen, such as the obvious cracking. The reason for this behavior is believed to be a function of the "art" of producing these sections and not to some basic difference in the specimens. Both specimens showed the same scalloped oxide/metal interface observed in the archive specimen (Figure 9). There was no apparent difference that could suggest oxidative corrosion occurred during the experiment. Any corrosion that occurred was either too small or proceeded just like the in-reactor oxidation that produced the original oxide film. Additional thinning of the specimen by ion milling produced some small areas of suitably-thinned oxide film for TEM and electron diffraction evaluation (Figures 15 and 16). The phase indicated by the electron diffraction patterns is monoclinic zirconia. The TEM micrographs show a texture that is indistinguishable from that observed in the archive specimen. The conclusion is that any change that has occurred has been too small to detect or is no different than the oxidative corrosion that occurs in reactors.

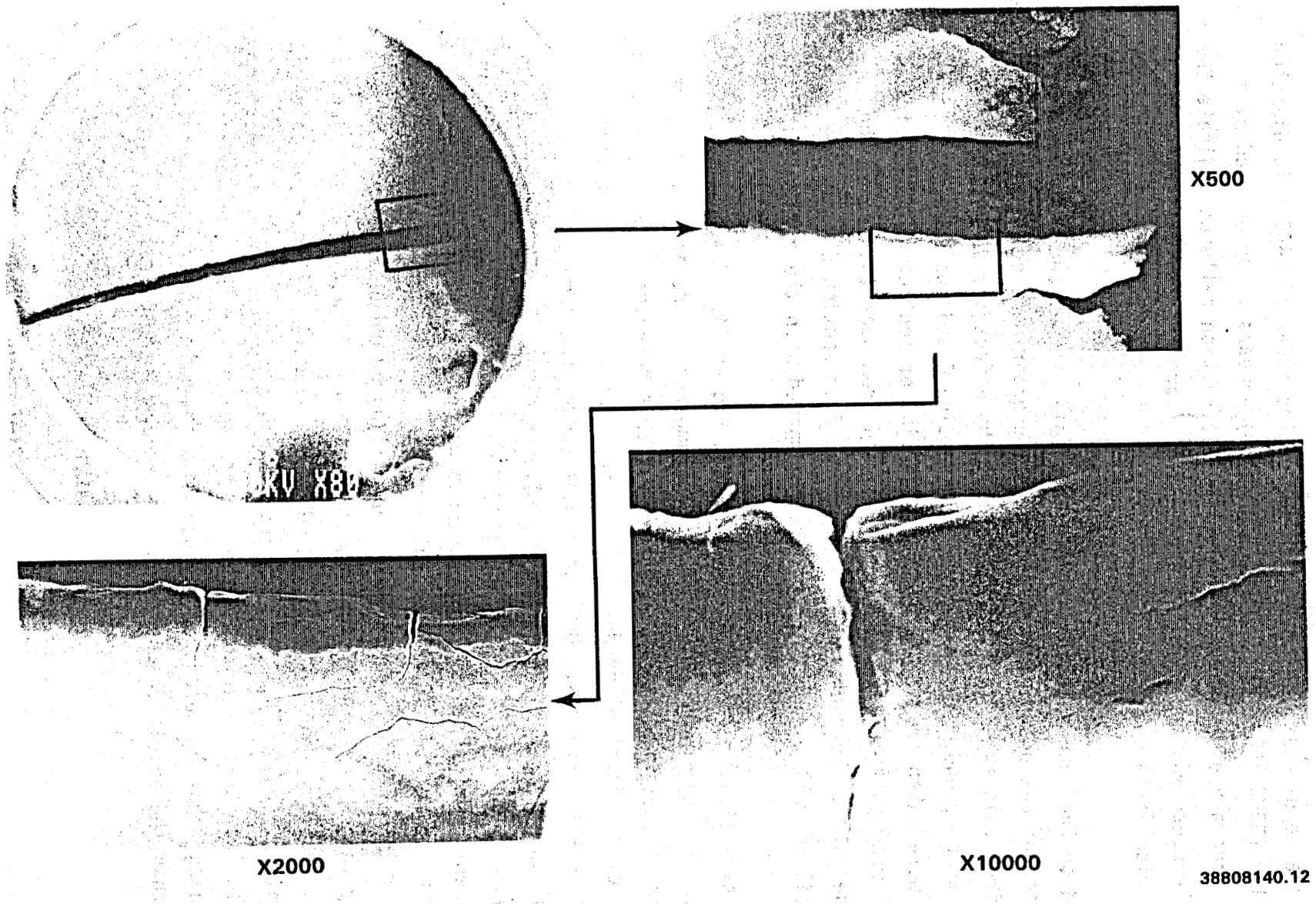

FIGURE 14. Appearance of Samples from Section E from the 12-Month Experiment After the First Cycle of Milling. (Milling is causing the material to crack. This as not observed with the archive; however, it is believed to be a milling problem and not due to a change in the material. Note that the mount includes two pieces of cladding placed so that the O.D. of one rests against the I.D. of the other.)

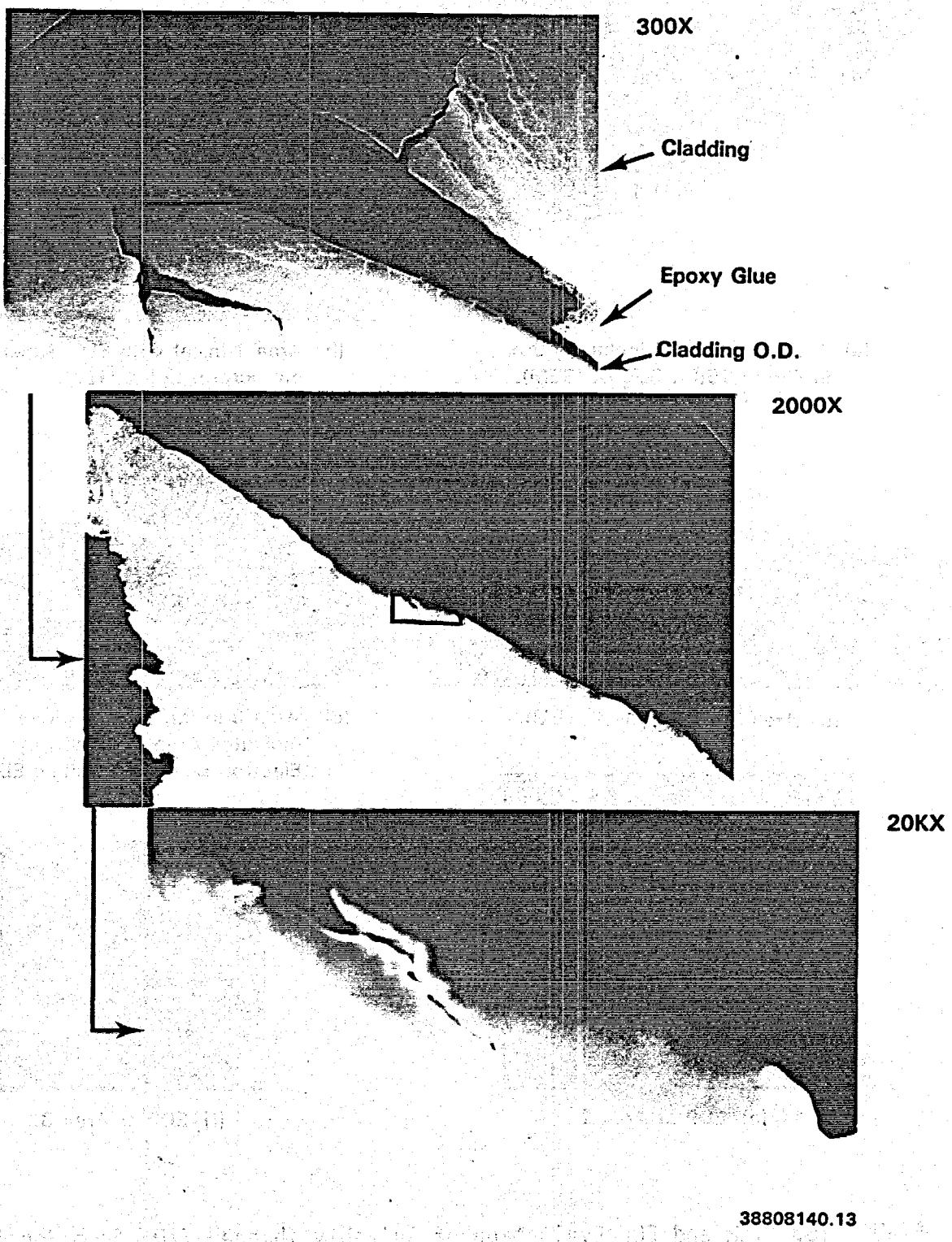

FIGURE 15. Area Similar to that Shown in Figure 14 After Additional Milling to Produce Areas of Ultra-thin Oxide for TEM Evaluation. (Much of the oxide has been milled off, leaving patches of thinned oxide attached to the metal substrate.)

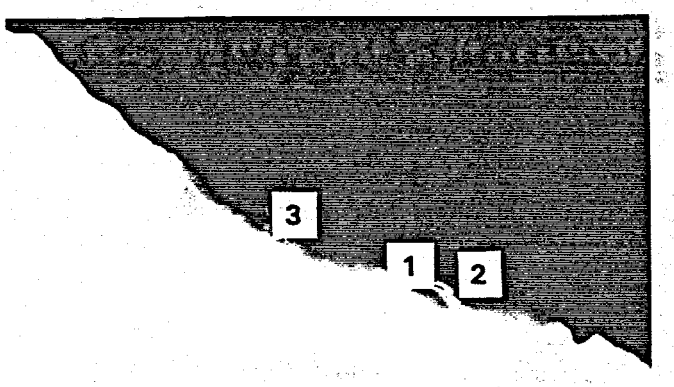

(a) Area Around and Including Box in Figure 15(b), 5000X (SEM).

(b) Area 1 in (a) with EDP Superimposed on Picture, 50KX (TEM).

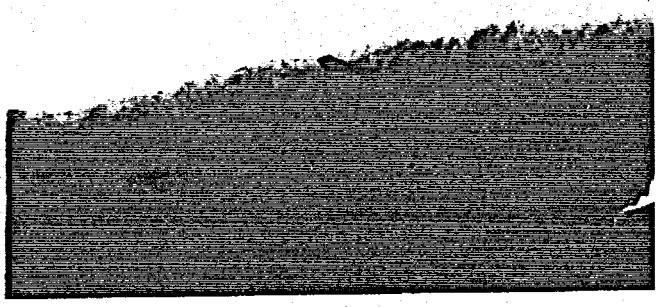

(c) Area 2 in (a), 50KX (TEM).

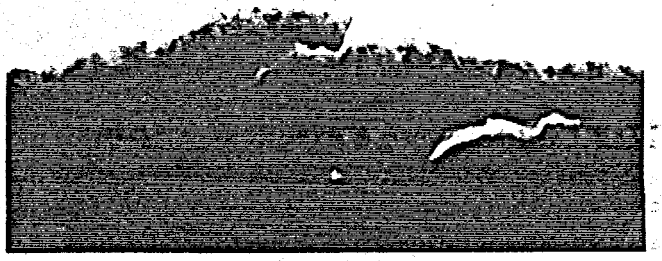

(d) Area 3 in (a), Lighter Circle Indicates Area Irradiated by Electron Beam to Produce EDP (TEM).

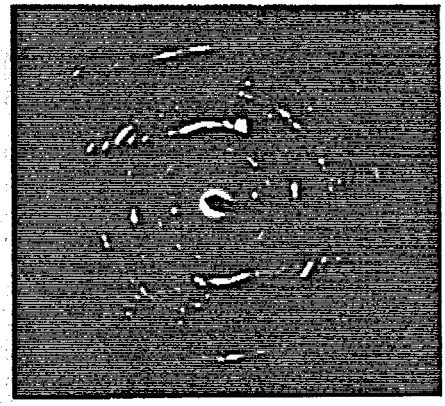

(e) EDP at Area 2.

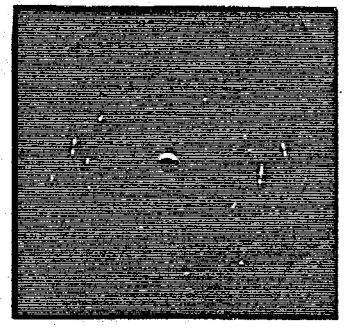

(f) EDP at Area 3.

38808140.14

FIGURE 16. TEM and EDP Evaluation of Suitably Thinned ZrO_2 from Section E from the 12-Month Experiment. (Note there is an image reversal between the SEM and the TEM micrographs. Barred pattern on (e) may either be due to columnar structure of the ZrO_2 or to electron transmission through thin metal.)

What are the expected changes in the oxide film as the result of the experiment if they are the same as those occurring in the reactor? Using the posttransition formula for the thickening of an oxide film on a Zircaloy given by Rothman[1]:

$$\Delta W(T,t) = \Delta W_t + 1.12 \times 10^8 \, EXP[-12{,}529/T] \cdot (t - t_t)$$

where:

ΔW = Change in weight (mg/100 cm^2)
W_t = Change in weight (mg/100 cm^2 at the transition point)
T = Temperature (°K)
t = Exposure time (days)
t_t = Time to transition (days).

one can calculate the expected thickening of a posttransition oxide film in 1 yr, i.e.,

$$(\Delta W(T = 363K,\ t + 365\ d) - \Delta W_t) - (\Delta W(T = 363K, t) - \Delta W_t)$$
$$= 1.12 \times 10^8 \, EXP[-12529/363] \times 365$$
$$= 1.12 \times 10^8 \times 1.024 \times 10^{-15} \times 365$$
$$= 4.18 \times 10^{-5} \text{ mg/100 } cm^2$$

Since the formation of 1 μm (10,000 Å) of ZrO_2 results in a weight change of 22 mg/100 cm^2, a weight change of 4.18×10^{-5} mg/100 cm^2 is equivalent to the formation of only 0.019 Å of oxide.

Obviously, this experiment was not set up as an attempt to detect homogeneous corrosion if it was expected to be as small as the above calculation suggests. It was set up to look for anomalous corrosion behavior not suggested by work already performed at higher temperatures but would occur as a result of environmental conditions characteristic of geometrics and materials associations found in a tuff repository. The corrosion behavior might include anything from more rapid homogeneous corrosion to various kinds of localized corrosion due to contact points, cladding defects, etc. The results of these experiments did not indicate greater than expected homogeneous corrosion or the occurrence of localized corrosion.

This page intentionally blank.

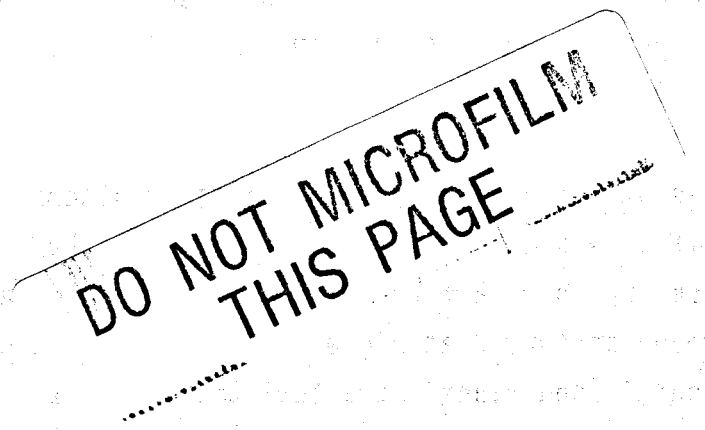

V. DISCUSSION AND CONCLUSIONS

A. LIMITS ON THE RATES OF GENERALIZED CORROSION

The objectives of this scoping experiment were to look for the effects of electrochemical corrosion when Zircaloy-4 spent fuel cladding was exposed to tuff-equilibrated Well J-13 water under potential tuff repository conditions and to explore/evaluate the techniques for observing/identifying/measuring the effects of corrosion on spent fuel cladding.

In most studies of corrosion of a material, coupons of the material are prepared and well characterized prior to the experiment so that changes can be readily identified and characterized via weight changes and microscopy. In this experiment, this kind of precharacterization was not possible because it would have denatured the specimen so that it would not have been characteristic of spent fuel cladding. To identify corrosion in this experiment was difficult because water environment corrosion had already been active for several years on the material (i.e., in reactor) so that the problem was one of identifying a small amount of additional corrosion on top of that which had already occurred. However, it was thought that since the repository environment was at a lower temperature and had a different water chemistry any corrosion that did occur might have a different texture and might be localized to areas around defects in the oxide film already present. In addition, weight change could not be employed as an indicator of corrosion because with a (sometimes porous) oxide film present, weight gains or losses could be due to precipitation in the porosity or on the surface of the oxide, or to spallation of the film. Therefore, the postexperiment sample evaluation was confined to macroscopic examination of the cladding specimens, to metallographic and SEM evaluation of polished sections of cladding specimens and, finally, to a detailed evaluation of several cladding specimens as ultra-thin sections using TEM, SEM, and electron diffraction.

As shown from the results, these methods could not identify a single feature on any of the cladding specimens that suggested that measurable corrosion had taken place during any of the experiments. However, these

results do allow an estimate of the maximum amount of corrosion to be made based on each observation as summarized in Table 5. Based on oxidation rates extrapolated to the temperature of the experiment (90 °C),[1] it was calculated that significantly less than an atom thickness of corrosion would have occurred in the already oxidized cladding, consistent with the fact that none was identified. The TEM and electron diffraction studies of the oxide film also suggested no effect from the exposure to the simulated repository environment in that no changes were detected in the crystal structure, grain size, or phases present.

TABLE 5

SUMMARY OF MAXIMUM CORROSION RATES
ESTIMATED FROM POSTEXPERIMENT OBSERVATIONS

Observation	(μm per yr)	Comments
No change in distribution of pre- and posttransition oxide film	<0.1	Complete transition takes place with a thickness change of about 0.4 μm, but noticeable changes in the relative distribution take place with much less implied thickness change.
Metallography/SEM	<1.0	Though no changes could be identified, if the oxide film formed during the experiment appeared the same as that already present, changes smaller than a micron could not be identified because of prior variations in oxide thickness, etc.
TEM/EDP	≲0.1	Would expect grain size at interface of oxidative corrosion product to be considerably smaller than that produced under reactor conditions. No very fine-grained layer observed.

As already mentioned, the model for oxidative corrosion at 90 °C predicts unmeasurable corrosion will occur in areas of cladding with already intact oxide films. However, the same model predicts that a film on the order of 150 Å would form on a bare metal surface at 90 °C in 1 yr and about 1000 Å would form at 170 °C (also in 1 yr) whereas an already established film would grow at about 10 Å per yr at 170 °C, a thickness change that is still undetectable. It is concluded from these observations that future experiments should include areas of polished metal on each cladding specimen and this has been incorporated into subsequent experiment plans.[11,12] These will provide areas that will undergo oxidative corrosion at a rate that should be measurable via Auger/ion mill chemical profiling. Polished areas are legitimate modifications to the material because they simulate abraded areas that might be produced on rods during consolidation and transport. Comparison between measured and calculated rates will indicate the applicability of the model to the repository environments. Unless a much greater oxidative corrosion rate than predicted by the model is observed, it is useless to look for corrosion effects via some microscopic method. If the model predicts the actual corrosion rate within a factor of 500, the cladding will not fail within the first 10,000 yr in a tuff repository by homogeneous cladding corrosion, i.e., the cladding is ~6 x 10^6 Å thick and at <90 °C it corrodes via oxidation <1 Å per yr according to the model.

B. CARBON-14 RELEASE FROM ZIRCALOY CLADDING

The only observed reaction of the cladding with the tuff-equilibrated Well J-13 water was its release of carbon-14 into the water. These measurements, begun late in the experiments, indicated measurable carbon-14 release to the water of ~180 dpm/mL (disintegrations per minute per milliliter of solution) (see Table 4). It appears that a carbon-14 concentration giving ~180 dpm/mL was close to a steady-state concentration which built up in the Well J-13 water. Similar solutions from the 2-mo and 6-mo experiments progressively lost carbon-14 when out of contact with the cladding bundles, apparently by exchange with the atmosphere.

If it was known how carbon-14 was distributed in the cladding and what form it is in, it could be used as an indicator of the interaction of the cladding environment with the cladding. It is believed that much of the inventory of carbon-14 in the cladding is at or near the surface, based on several etching experiments (i.e., a piece of cladding for which 10% of the weight was etched away from the interior and exterior surfaces lost 90% of its carbon-14 activity). Other specimens lightly etched only on the outside surfaces lost up to three-fourths of their original activity. Without detailed information with respect to the distribution and state of the carbon-14 in the cladding, it is impossible to accurately interpret its release into the Well J-13 water used in these scoping experiments. Experiments to characterize the inventory and distribution of carbon-14 are planned and initial scoping tests are already in progress.

One possible interpretation of the carbon-14 values observed in these experiments is as follows. It is assumed that ~80% of the cladding carbon-14 inventory is entrained in the oxide film on the outside surface of the cladding, that the carbon-14 is being released at some approximately constant rate to the Well J-13 water, and that the carbon-14 is being lost (i.e., by exchanging with carbon-12 from the atmosphere in the form of CO_2) at some rate proportional to the concentration of carbon-14 in the Well J-13 water. The following equation can be used to describe the time variation of carbon-14 in the Well J-13 water:

$$dC/dt = A - BC$$

where:

C = Concentration

t = Time

A = Constant release rate from the cladding

B = Constant relating release rate from the solution to the atmosphere as a function of concentration.

Solving for C as a function of time results in the following equation which gives the time variation of the carbon-14 concentration in Well J-13 water:

$$C = A/B\ (1 - e^{-Bt}),\ \text{where } A/B = Co, \text{ the steady-state concentration.}$$

Fitting that equation to the "data":

$$\frac{165}{2.22 \times 10^{12}}\ \text{dpm/mL} = 7.4 \times 10^{-11}\ \text{Ci/mL at } t = 97\ \text{d}$$

$$\frac{180}{2.22 \times 10^{12}}\ \text{dpm/mL} = 8.1 \times 10^{-11}\ \text{Ci/mL at } t = 170\ \text{d}$$

gives:

$$C = 8.25 \times 10^{-5}\ \mu\text{Ci/mL}(1 - e^{-0.0238t})$$

where:

C = Concentration of carbon-14 in μCi/mL as a function of time
Co = 8.25×10^{-5} μCi/mL
t = Time
B = 0.0238 the proportion of the inventory in solution that leaves the Well J-13 water each day.

According to the "model," (0.0238 x 361) = 8.6 inventories of carbon-14 have entered and/or passed through the Well J-13 water during the course of the 12-mo (361-d) experiment. An inventory is equal to the average concentration in the Well J-13 water (~8.0×10^{-5} μCi/mL) times the volume of Well J-13 water (~50 mL) which equals 4.0×10^{-3} μCi of carbon-14. Therefore the total removed from the cladding is 8.6 times that or 3.3×10^{-2} μCi. The amount expected to be found in the oxide film contacted by Well J-13 water according to the assumption of 80% of the cladding inventory located in the oxide film is ~27 μCi. This suggests that about 0.1% of the total oxide film inventory

has been "leached" from the oxide in 1 yr. If the carbon-14 is uniformly distributed through the oxide film depth (~10 μm), this would be equivalent to the inventory in the top ~100 Å of the oxide film. This result suggests again that there has been very little interaction between the spent fuel cladding and the simulated tuff repository environment.

It is clear that the final interpretation of the carbon-14 release data is highly dependent on our understanding of its distribution and chemical state in the cladding. It is also clear, because of its detectability, that it has considerable potential as an indicator of the interaction of the environment with spent fuel cladding. Its real value and the best way to exploit it will only be known after its distribution and chemical state in the cladding have been determined. Note that these features are also critical in the proper management of carbon-14 as one of the radionuclides that must have its release rate controlled according to the limits set in NRC rule 10 CFR 60.113.

C. CONCLUSIONS

1. Metallography and standard SEM techniques did not identify any kind of corrosion (homogeneous or localized) on Zircaloy-4 spent fuel cladding in contact with tuff-equilibrated Well J-13 water at ~90 °C for up to 1 yr. Prepolishing part of the cladding surface would greatly enhance the probability of identifying localized corrosion by microscopic methods after a test.

2. If the model for aqueous oxidative corrosion of zirconium and its alloys summarized by Rothman[1] can be extrapolated to 90° and 170 °C, then metallographic techniques and SEM are not sensitive enough to observe homogeneous corrosion on spent fuel cladding. However, Auger/ion milling techniques should be able to measure oxidative corrosion films that would develop on polished surfaces.

3. The TEM, SEM, and electron diffraction were used to characterize ultra-thin sections of cladding from the 12-mo experiment and archived cladding material from the same fuel rod, but were unable to detect any differences between them believed to be due to corrosion. It is recommended, however, that these techniques be applied to material from the 170 °C autoclave tests when they become available.

4. Carbon-14 is expected to be a valuable indicator of cladding interaction with the environment once its distribution and state in the cladding is well understood and described.

This page intentionally blank.

VI. REFERENCES

1. A. J. Rothman, Potential Corrosion and Degradation Mechanisms of Zircaloy Cladding on Spent Nuclear Fuel in a Tuff Repository, UCID-20172, Lawrence Livermore National Laboratory, Livermore, CA, September 1984.

2. H. D. Smith, Zircaloy Cladding Corrosion Degradation in a Tuff Repository, HEDL-7455, Rev. 1, Hanford Engineering Development Laboratory, Richland, WA, July 1985.

3. H. D. Smith, Zircaloy Spent Fuel Cladding Electrochemical Corrosion Scoping Experiment, HEDL-TC-2562, Hanford Engineering Development Laboratory, Richland, WA, December 1984.

4. V. M. Oversby, The Reaction of Topopah Spring Tuff With J-13 Water at 150 °C - Samples from Drill Cores USW G-1, USW GU-3, USW G4, and UE-25h#1, UCRL-53629, Lawrence Livermore National Laboratory, Livermore, CA, March 1985.

5. R. B. Davis and V. Pasupathi, Data Summary Report for the Destructive Examination of Rods G7, G9, J8, I9, and H6 from Turkey Point Fuel Assembly B17, HEDL-TME 80-85, Hanford Engineering Development Laboratory, Richland, WA, April 1981.

6. Teledyne Wah Chang Albany, Information Brochure TWCA-8102ZR, Teledyne Wah Chang Albany, Albany, Oregon.

7. H. D. Smith, Spent Fuel Cladding Characteristics and Choice of Experimental Specimens for Cladding Corrosion Evaluation Under Tuff Repository Conditions, HEDL-TC-2530, Hanford Engineering Development Laboratory, Richland, WA, November 1984.

8. R. E. Einziger and J. A. Cook, Pre-test Visual Examination and Crud Characterization of LWR Rods Used in the Long-Term, Low-Temperature Whole Rod Test, NUREG/CR-3285, HEDL-TME 83-9, Hanford Engineering Development Laboratory, Richland, WA, March 1984.

9. A. B. Johnson et al., "Nature of Deposits on BWR and PWR Primary System Surfaces in Relation to Decontamination," Water Chemistry II, Brit. Nuc. Eng. Soc. and Royal Soc. of Chem., Bournemouth, October 14-17, 1980.

10. G. Thomas and M. J. Goringe, "Transmission Electron Microscopy of Materials," pp. 110-111, Wiley, 1979.

11. X-Ray Powder Diffraction File(s), 24-1165 13-307, compiled by JCPDS-International Committee on Diffraction Data, 1501 Parklane, Swarthmore, PA 19081.

12. H. D. Smith, Zircaloy Spent Fuel Cladding Electrochemical Corrosion Experiment at 170 °C and 120 PSIA H2O, HEDL-7545, Hanford Engineering Development Laboratory, Richland, WA, April 1986.

EXTERNAL DISTRIBUTION

DOE-HQ/Office of Civilian
Radioactive Waste Management (13)
Forrestal Building
Washington, DC 20585

CE Kay, Acting Director	RW-1
DH Alexander	RW-332
JC Bresee	RW-10
SJ Brocoum	RW-221
VJ Cassella	RW-123
MW Frei	RW-22
BG Gale	RW-23
TH Isaacs	RW-40
SH Kale	RW-20
G. Parker	RW-333
JD Saltzman	RW-20
S. Rousso	RW-10
R. Stein	RW-30

DOE/Nevada Operations Office (23)
P.O. Box 98518
Las Vegas, NV 89193-8518

M. Blanchard, WMPO
CP Gertz, Project Manager, Waste Management PO MS-523 (5)
CL West, Director, Office of External Affairs
JL Fogg, Technical Information Office (12)
PK Fitzsimmons, Director, Health Physics & Envir. Div.
LP Skousen, WMPO
M. Valentine, WMPO
M. Cloninger

DOE-RL/Office of Asst Manager
for Research and Projects (3)
P.O. Box 550
Richland, WA 99352

DC Langstaff, General Engineer	A5-90
DH Dahlen, Chief, BWIP Branch	A5-10
Public Reading Room	A1-65

DOE/Office of Scientific
and Technical Information
Science and Technology Division
P.O. Box 62
Oak Ridge, TN 37831

AT Tamura

Argonne National Laboratory (2)
Chemical Technology Division
9700 S. Cass Avenue, Bldg. 205
Argonne, IL 60439

J. Bates
E. Veleckis

Battelle Columbus Laboratory
505 King Avenue
Columbus, OH 43201

ONWI Library

Berkeley Nuclear Laboratories
Berkeley, Glouscestershire
GL 13 9PB, UK

KA Simpson, Section Leader

Brookhaven National Laboratory
Associated Universities, Inc.
Upton, NY 11973

D. Schweitzer

Center for Nuclear
Waste Regulatory Analysis
6220 Culebra Road
Drawer 28510
San Antonio, TX 78284

Director

EXTERNAL DISTRIBUTION (Cont'd)

City of Boulder City
P.O. Box 367
Boulder City, NV 89005

Director, Community Planning

City of Caliente (5)
P.O. Box 158
Caliente, NV 89008

J. Foremaster

City of Henderson
Henderson, NV 89015

City Manager

City of Las Vegas
400 E. Stewart Avenue
Las Vegas, NV 89101

Economic Development Dept

City of North Las Vegas
P.O. Box 4086
North Las Vegas, NV 89030

Community Planning & Development

Clark County
225 Bridger Avenue, 7th Floor
Las Vegas, NV 89155

Comprehensive Planning Dept

Commission of the European Communities
Rue de la Loi 200
B-1049 Brussels, Belgium

Desert Research Institute
Water Resources Center
P.O. Box 60220
Reno, NV 89506

J. Fordham

Desert Research Institute
Water Resources Center
2505 Chandler Avenue, Suite 1
Las Vegas, NV 89120

M. Mifflin

EG&G Energy Measurements, Inc.
P.O. Box 1912
Las Vegas, NV 89125

E. Ezra, Manager, NNWSI GIS,
MS H-02

Fenix & Scisson, Inc.
Las Vegas Branch
P.O. Box 93265
Las Vegas, NV 89193-3265

JA Cross, Manager MS-514

Fenix & Scisson, Inc.
101 Convention Center Drive, Suite 320
Las Vegas, NV 89109

RL Bullock, NNWSI Tech
Project Officer MS-403

Hahn Meitner Institut GmbH
Glienickerstr. 100
D-1000 Berlin 39
Federal Republic of Germany

Bernd Grambow

EXTERNAL DISTRIBUTION (Cont'd)

Holmes & Narver, Inc.
Energy Support Division
P.O. Box 93838
Las Vegas, NV 89193-3838

AE Gurrola, General Manager MS-580

Holmes & Narver, Inc.
101 Convention Center Drive, Suite 860
Las Vegas, NV 89109

JC Calovini, NNWSI Technical Project Officer

Lawrence Berkeley Laboratory
Field Systems
Bldg 50B/4235
Berkeley, CA 94720

EP Binnall, Group Leader

Lawrence Livermore
National Laboratory (66)
P.O. Box 808
Livermore, CA 94550

R. Aines	L-219
L. Ballou	L-206
W. Bourcier	L-219
C. Bruton	L-219
B. Bryan	L-206
J. Dronkers	L-204
D. Emerson	L-204
W. Glassley	L-204
K. Jackson	L-204
J. Kass	L-204
K. Knauss	L-202
D. Lappa	L-196
W. Lin	L-201
C. Merzbacher	L-202
W. O'Connell	L-195
V. Oversby	L-206
C. Poppe	L-231
A. Ramirez	L-204
L. Ramspott (3)	L-204
M. Revelli	L-206

Lincoln County
P.O. Box 90
Pioche, NV 89043

Lincoln County Commission

Los Alamos National Laboratory (5)
P.O. Box 1663
Los Alamos, NM 87545

K. Eggert
DT Oakley, NNWSI Technical Project Officer (4) J-521

Los Alamos National Laboratory
101 Convention Center Drive, Suite P230
Las Vegas, NV 89109

HN Kalia, Manager, Exploratory Shaft Test MS-527

Mountain West Research-Southwest, Inc.
432 North 44th Street, Suite 400
Phoenix, AZ 85008

E. Anderson

E. Russell	L-197
R. Ryerson	L-201
W. Sawka	L-202
R. Schock	L-209
L. Schwartz	L-203
H. Shaw (17)	L-204
D. Short	L-204
R. Silva	L-396
R. Stout	L-200
H. Tewes	L-204
A. Tompson	L-206
R. Van Konynenburg	L-370
B. Viani	L-219
H. Weed	L-201
A. Wijesinghe	L-200
T. Wolery	L-219
J. Yow	L-206
L. Younker	L-209
NWM Library (10)	L-204

EXTERNAL DISTRIBUTION (Cont'd)

National Bureau of Standards (2)
Division 450
Gaithersburg, MD 20899

C. Interrante Bldg 223/Rm A-245

Nuclear Regulatory Commission (4)
Division of Waste Management
Washington, DC 20555

M. Bell MS-WFI-4-H3
Chief, Repository Proj Branch
Document Control Center
NTS Section Leader

Nuclear Regulatory Commission
1050 East Flamingo Road, Suite 319
Las Vegas, NV 89119

PT Prestholt, Site Rep

Nye County
P.O. Box 153
Tonopah, NV 89049

Planning Dept

Reynolds Electrical
& Engineering Co, Inc. (2)
P.O. Box 98521
Las Vegas, NV 89193-8521

DL Fraser, Gen Mgr MS-555
RF Pritchett, NNWSI Tech MS-615
Project Officer

Royal Institute of Technology
Department of Inorganic Chemistry
S-100 44 Stockholm 70, Sweden

Jordi Bruno

Sandia National Laboratories (7)
P.O. Box 5800
Albuquerque, NM 87185

TO Hunter, NNWSI Tech
Project Officer (5) Org 6310
RW Lynch Org 6300
S. Sinnock

Savannah River Laboratory (2)
Aiken, SC 29808

B. Kitchen Bldg 773-41A
J. Plodinec Bldg 773-A, Rm B-120

Science Applications
International Corporation (3)
1626 Cole Boulevard, Suite 270
Golden, CO 80401

TG Barbour

Science Applications
International Corporation (3)
101 Convention Center Drive, Suite 407
Las Vegas, NV 89109

SAIC-T&MSS Library (2)
ME Spaeth, NNWSI Tech
Project Officer

State of Nevada
Office of the Governor
Capitol Complex
Carson City, NV 89710

T. Hay, Exec Assistant

EXTERNAL DISTRIBUTION (Cont'd)

State of Nevada (4)
Nuclear Waste Project Office
Evergreen Center, Suite 252
1802 N. Carson Street
Carson City, NV 89701

CH Johnson, Tech Prog Mgr
RR Loux Jr., Exec Director (3)

Studsvik AB
S-611 82 Nyköping, Sweden

RW Forsyth

Svensk Karnbranslehantering AB
Box 5864
S-102 48 Stockholm, Sweden

Dr. Lars Werme

Systems Support Inc.
P.O. Box 1432
Manassas, VA 22110

R. Moler

University of California
Dept. of Nuclear Engineering
Berkeley, CA 94720

TH Pigford

U.S. Geological Survey (7)
P.O. Box 25046
421 Federal Center
Denver, CO 80225

VW Glanzman Rm 913
LR Hayes, NNWSI Tech
Project Officer (6)

U.S. Geological Survey
Engineering Geology
106 National Center
12201 Sunrise Valley Drive
Reston, VA 22092

JR Rollo, Deputy Asst Dir

Technical Research Centre of Finland
Reactor Laboratory
Otakaari 3A
SF-02150 Espoo 15, Finland

Kaija Ollila

Roy F. Weston, Inc. (3)
955 L'Enfant Plaza SW, Suite 800
Washington, DC 20024

E. Benz N Bldg NW
WM Hewitt, Prog Manager
Technical Information Center

West Valley Nuclear Services Co, Inc.
Process Technology & Testing
P.O. Box 191
West Valley, NY 14171-0191

J. Pope, Manager

Whiteshell
Nuclear Research Establishment (8)
Atomic Energy of Canada Ltd.
Pinawa, Manitoba ROE 1LO, Canada

C. Davison, GWT Branch
K. Dormuth, FWT Branch
L. Johnson, FWT Branch
FP Sargent
D. Shoesmith, RC Branch
G. Simmons, FWT Branch
S. Stroes-Gascoyne, FWT Branch
S. Sunder, RC Branch

INTERNAL DISTRIBUTION

Pacific Northwest Laboratories (40)
P.O. Box 999
Richland, WA 99352

MJ Apted	P7-14
WW Ballard	K1-78
TT Claudson	K1-45
RE Einziger	P7-14
WJ Gray	K2-38
ED Jenson	P7-22
MR Kreiter	P7-14
AC Leaf	P7-22
SC Marschman	P7-14
JE Mendel	P7-18
MD Merz	K3-59
PW Reimus	P7-14
PF Salter	K2-35
JW Shade	K2-38
HD Smith (20)	P7-14
RT Steele	P7-22
RW Stromatt	P7-22
JR Stuart	P7-14
LE Thomas	P8-13
NH Uziemblo	P8-13
CN Wilson	P7-14

Westinghouse Hanford Co. (9)
P.O. Box 1970
Richland, WA 99352

DG Farwick	S1-52
GT Harper	H9-19
RL Knecht	L5-59
W. Yunker	L4-51
BWIP Library (2)	H9-16
Documentation (3)	L8-15